ACS OMEGA

Open Access

http://pubs.acs.org/journal/acsodf

Article

In Vivo Proximity Cross-Linking and Immunoprecipitation of Cell Wall Epitopes Identify Proteins Associated with the Biosynthesis of Matrix Polysaccharides

Pitchaporn Wannitikul, Issariya Dachphun, Jenjira Sakulkoo, Anongpat Suttangkakul, Passorn Wonnapinij, Rachael Simister, Leonardo D. Gomez, and Supachai Vuttipongchaikij*

Cite This: *ACS Omega* 2024, 9, 31438−31454

Read Online

ACCESS | Metrics & More | Article Recommendations | Supporting Information

ABSTRACT: Identification of proteins involved in cell wall matrix polysaccharide biosynthesis is crucial to understand plant cell wall biology. We utilized *in vivo* cross-linking and immunoprecipitation with cell wall antibodies that recognized xyloglucan, xylan, mannan, and homogalacturonan to capture proteins associated with matrix polysaccharides in *Arabidopsis* protoplasts. The use of cross-linkers allowed us to capture proteins actively associated with cell wall polymers, including those directly interacting with glycans via glycan−protein (GP) cross-linkers and those associated with proteins linked to glycans via a protein−protein (PP) cross-linker. Immunoprecipitations led to the identification of 65 *Arabidopsis* protein IDs localized in the Golgi, ER, plasma membrane, and others without subcellular localization data. Among these, we found several glycosyltransferases directly involved in polysaccharide synthesis, along with proteins related to cell wall modification and vesicle trafficking. Protein interaction networks from DeepAraPPI and AtMAD databases showed interactions between various IDs, including those related to cell-wall-associated proteins and membrane/vesicle trafficking proteins. Gene expression and coexpression analyses supported the presence and relevance of the proteins to the cell wall processes. Reverse genetic studies using T-DNA insertion mutants of selected proteins revealed changes in cell wall composition and saccharification, further supporting their potential roles in cell wall biosynthesis. Overall, our approach represents a novel approach for studying cell wall polysaccharide biosynthesis and associated proteins, providing advantages over traditional immunoprecipitation techniques. This study provides a list of putative proteins associated with different matrix polysaccharides for further investigation and highlights the complexity of cell wall biosynthesis and trafficking within plant cells.

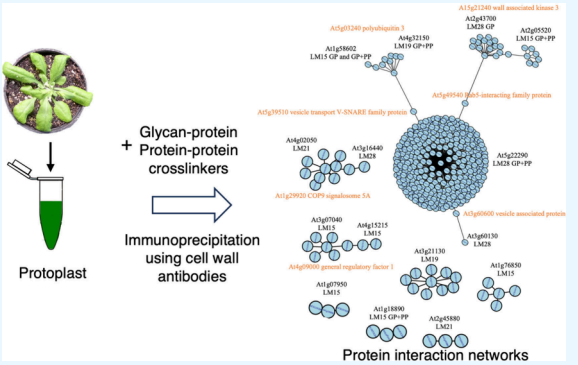

INTRODUCTION

Plant cell wall biosynthesis is a complex and coordinated process, with numerous enzymes and regulatory proteins playing pivotal roles.[1] Unlike cellulose, which is synthesized from the cell membrane toward the cell wall, matrix polysaccharides undergo synthesis and modification in the Golgi apparatus before being transported to the cell walls through vesicles for final assembly.[2−4] However, precise molecular mechanisms underlying cell wall biosynthesis and remodeling are not fully understood. Many proteins and enzymes involved in various stages of this biosynthetic pathway present challenges for a comprehensive identification of the biosynthesis components.[5] While glycosyltransferases, as the primary biosynthesis enzymes for matrix polysaccharides, have been extensively studied and characterized, we have little knowledge about the complete set of proteins involved in processes such as side chain substitutions, polysaccharide delivery associated with membrane or vesicles, and regulatory proteins.[6] Therefore, it is important to identify and characterize these associated proteins to understand plant cell wall biosynthesis, from glycan synthesis to delivery and wall assembly.

Plant cell wall matrix polysaccharides comprising hemicelluloses and pectins represent a diverse group of polysaccharides that play essential roles in maintaining cell wall integrity and function.[7,8] Xyloglucan (XyG), a major hemicellulose found in primary cell walls of dicots and nongraminaceous monocots, contributes to cell wall strength and elasticity through interactions with cellulose microfibrils. Structurally, xyloglucans consist of a β-1,4-linked glucan backbone, which is similar to cellulose, with side chains composed of xylose residues attached to the backbone at regular intervals. These

Received: January 18, 2024
Revised: June 21, 2024
Accepted: June 27, 2024
Published: July 11, 2024

xylose residues can be further substituted with other monosaccharides, such as galactose and fucose, forming a diverse array of xyloglucan structures.[9] Xylans, which can have a wide range of structural arrangements including glucuronoxylan (GX), glucuronoarabinoxylan (GAX), and arabinoxylan (AX), are prominent hemicelluloses found in the secondary cell walls of many plant species. In some species, xylans can also be found in the primary cell walls of GX. GX is abundant in the secondary cell walls of dicots and the primary and secondary walls of grasses, with a structure comprising a backbone of β-1,4-linked xylose residues and occasional glucuronic acid substitutions, conferring rigidity to the cell wall. GAX and AX are characterized by the presence of arabinose and glucuronic acid side chains, which influence their functionality and interaction with other cell wall components.[10] Mixed linkage glucan (MLG), a common hemicellulose (after xylan), is found in the primary cell walls of many grass species. MLG is characterized by a mixed β-1,3 and β-1,4-glucan backbone, contributing to the flexibility and strength of grass cell walls.[10] Galactomannan (GM), prevalent in the primary cell walls of monocots, is characterized by a β-1,4-linked mannose backbone with galactose side chains.[11] On the other hand, pectins are structurally and functionally the most complex polysaccharides in plant cell walls, encompassing a family of galacturonic acid-rich polymers including homogalacturonan (HGA), rhamnogalacturonan I (RG-I), rhamnogalacturonan II (RG-II), and xylogalacturonan (XGA).[12,13] These polysaccharides have pivotal roles in cell wall integrity, plant growth, morphology, development, and defense. Furthermore, these matrix polysaccharides undergo modifications such as methyl and acetyl substitutions right upon biosynthesis for their functionality.[12,14,15] For instance, recent work has shown that QUASIMODO2 (QUA2) is a pectin methyltransferase required for normal pectin biosynthesis, which is crucial for their roles in maintaining cell wall integrity.[16]

In recent years, efforts have been made to identify and characterize proteins associated with plant cell wall biosynthesis. Zhou et al.[17] investigated protein interactions related to cell wall synthesis and found 100 protein candidates and selected 42 of them as the most reliable candidates for future study. Parsons et al.[18] utilized a combination of density centrifugation and surface charge separation to isolate Golgi membranes from *Arabidopsis*, enabling proteomic analysis that led to the identification of 371 proteins localized in the Golgi and involved in matrix polysaccharide biosynthesis. Cai et al.[19] employed microarray data and coexpression networks in Populus to identify gene candidates associated with plant cell wall synthesis. Moreover, Atmodjo et al.[20] focused on the immunoprecipitation of the GAUT1/GAUT7 complex, responsible for homogalacturonan synthesis, and identified 12 proteins involved in this biosynthetic complex, including glycosyltransferases, glycosidases, and other cell wall-related proteins. In parallel, other studies have aimed to identify proteins functioning within the cell wall itself, known as extracellular proteomes or cell wall proteomes.[21] Interestingly, these investigations revealed the presence of noncanonical cell wall proteins, which were previously expected to reside in the endoplasmic reticulum (ER) or Golgi, indicating the complexity and diversity of the cell wall proteome. Collectively, these studies have provided an extensive list of proteins/genes involved in cell wall polysaccharide biosynthesis, including those directly participating in synthesis as well as those functioning indirectly or in close proximity to the synthetic complex.

Notably, many previous studies have utilized nonspecific approaches to identify proteins involved in cell wall biosynthesis, such as total purified Golgi fractions and proteomic analysis.[18] As a result, it is difficult to assign specific functions for these proteins to specific cell wall polysaccharides or other related processes. In light of this, our study aims to identify novel proteins involved in the biosynthesis of specific matrix polysaccharides, particularly during active synthesis within the cell. In this study, we devised a specific approach by using cell wall antibodies that recognized cell wall polysaccharides including XyG, GX, GM, and HGA. *Arabidopsis* protoplasts were used to ensure immunoprecipitation of cell wall epitopes occurring within the intracellular space. We treated the protoplasts with molecular cross-linkers to stabilize and capture proteins associated with matrix polysaccharides that are undergoing synthesis within the cells. Immunoprecipitation was then performed using glycan-specific monoclonal antibodies. Two types of cross-linkers were used, glycan−protein (GP) and protein−protein (PP) cross-linkers, to capture proteins both directly and indirectly associated with cell wall polymers. To verify the identified proteins, we conducted extensive analyses using a number of *Arabidopsis* gene databases, including those for subcellular localization, protein interactions, and gene expression and coexpression profiling. We identified candidate proteins that are directly or indirectly involved in the biosynthesis and delivery of four major plant cell wall matrix polysaccharides. Moreover, we selected three proteins for further investigation, analyzing T-DNA insertion mutants to assess their role in matrix polysaccharide synthesis. The proteins identified represent promising candidates for further investigation and potential modification aimed at enhancing cell wall matrix polysaccharides, which could lead to crop improvement and various biotechnological applications.

MATERIALS AND METHODS

Plant Materials and Growth Conditions. *Arabidopsis* Col-0 seeds were germinated on 1% (w v^{-1}) agar plates containing 1/2 strength Murashige and Skoog medium and 1% (w v^{-1}) sucrose for 7 days and then grown in compost under conditions: 16 h light (125 μmol photons m^{-2} s^{-1}) at 22 °C. The *Arabidopsis* Col-0 seeds (stock deposition number N1093) and T-DNA insertion lines (SALK_119422 for At2g43700, SALK_152917 for At5g12150, and SALK_203306C for At3g22460) were obtained from NASC (Nottingham *Arabidopsis* Stock Centre). All methods were performed in accordance with the relevant guidelines and regulations.

Protoplast Isolation. Protoplasts were isolated from leaves of 3-week-old plants using a modified version of the Tape−*Arabidopsis* Sandwich method.[22] The upper epidermal surface of the leaves was placed on a glass slide, while the lower epidermal surface was attached to a strip of transparent tape. The lower epidermal cell layer was carefully peeled off and transferred to a Petri dish containing an enzyme solution (1% cellulase, 0.25% macerozyme, 0.4 M mannitol, 10 mM $CaCl_2$, 20 mM KCl, 0.1% BSA, and 20 mM MES at pH 5.7). The Petri dish was then shaken at 40 rpm at 25 °C for 2 h. The resulting protoplasts were separated by centrifugation at 150 rpm for 10 min, washed twice with prechilled modified W5 solution (154 mM NaCl, 125 mM $CaCl_2$, 5 mM KCl, 5 mM glucose, and 2 mM MES at pH 5.7), and incubated on ice for

https://doi.org/10.1021/acsomega.4c00534
ACS Omega 2024, 9, 31438−31454

30 min. Finally, the protoplasts were resuspended in modified MMg solution (0.4 M mannitol, 15 mM $MgCl_2$, and 4 mM MES at pH 5.7) to obtain a final concentration of 5×10^6 cells mL^{-1}. Protoplast concentrations were determined using a hemocytometer.

Immunoprecipitation and Protein Identification by Liquid Chromatography−Mass Spectrometry (LC-MS/MS). Immunoprecipitation using glycan-specific antibodies was performed using *Arabidopsis* protoplasts treated with glycan−protein cross-linkers (GP) and glycan−protein and protein−protein cross-linkers (GP+PP). Protoplasts were aliquoted into three groups (10^6 cell each) before being added with GP cross-linkers, GP+PP cross-linkers, and a buffer with no cross-linker and incubated at 25 °C for 2 h. The GP cross-linkers were prepared by mixing MMg solution with 1 mM of KMUH, EMCH, BMPH, and MPBH. For GP+PP cross-linkers, the GP cross-linker solution was added with 1 mM BMOE. These cross-linkers were purchased from Thermo Fisher Scientific. Treated protoplasts were collected by centrifugation at 150 rpm for 10 min, and total proteins were extracted using HEPES protein extraction buffer (50 mM HEPES pH 6.8, 25 mM KCl, 0.25 mM $MnCl_2$, 0.25 mM $MgCl_2$, 2 mM EDTA, 40 mM CHAPs, 1X proteinase inhibitor, 1 mM PMSF, 50 mM DTT). After protein quantification using the Bradford assay, 1 mg of the total protein was used for immunoprecipitation using SureBeads protein G immobilized with cell wall specific antibodies including LM15, LM19, LM21, and LM28. Briefly, the magnetic beads were washed three times with PBST before incubation with an antibody (1:10 dilution with PBST) at room temperature for 1 h and then washed twice using PBS-T. The protein extract was added to the beads and incubated at room temperature for 1 h, followed by washing with PBS-T three times. The protein was eluted by incubating with 20 mM glycine pH 2.0 at room temperature for 5 min, and then 1 M phosphate buffer pH 7.4 was added to the protein. The eluted protein was briefly run in a 4% polyacrylamide stacking gel of SDS-PAGE, stained, and excised for LC-MS/MS analysis.

The gel band was subjected to in-gel trypsin digestion at 37 °C for 16 h. Peptides were extracted twice using a solution of 50% acetonitrile and 5% trifluoroacetic acid (TFA) and then dried in a vacuum centrifuge. Subsequently, peptides were reconstituted in 15 μL of 0.1% formic acid (FA) before analysis. The LC−MS/MS system comprised a liquid chromatography component (Dionex Ultimate 3000, Thermo Scientific) coupled with an electrospray ionization (ESI)/quadrupole ion trap mass spectrometer (model amazon SL, Bruker, Germany) at the Proteomics Services, Faculty of Medical Technology, Mahidol University (Salaya Campus), Nakonpathum, Thailand. LC separation was conducted on a reversed-phase column (Hypersil GoLD 50 × 0.5 mm, 5 μm C18) and safeguarded by a guard column (Hypersil GoLD 30 × 0.5 mm, 5 μm C18), with elution at a flow rate of 0.1 mL/min under gradient conditions of 5−80% B over 50 min. Mobile phase A consisted of water/formic acid (99.9:0.1, v/v), while mobile phase B consisted of acetonitrile. Mass spectral data ranging from 300 to 1500 m/z were collected in positive ionization mode. Peptide mass fingerprinting was conducted using the Swiss-Prot and *Arabidopsis thaliana* databases through the MASCOT searching engine (http://www.matrixscience.com). Search parameters in a MASCOT MS/MS iIon search included carbamidomethylation at cysteine residues as a fixed modification, oxidation at methionine residues as a variable modification, peptide tolerance of ±1.2 Da, MS/MS fragment tolerance of ±0.6 Da, and allowance for 1 missed trypsin cleavage site. Proteins with a Mascot score greater than the threshold, set with a p-value < 0.05, were considered significant.

Protein Identifications. The protein IDs were searched for *Arabidopsis* protein interactions using DeepAraPPI (based in deep learning-assisted prediction)[23] and AtMAD (based on experimental data such as FRET, yeast two-hybrid, coimmunoprecipitation, and affinity capture-MS).[24] For coexpression analysis, the *Arabidopsis* RNA-seq Database was used.[25] Protein interaction and coexpression networks were built using the igraph R package[26] (R Studio 2023.03.1 Build 446 2009−2023 Posit Software, PBC "Cherry Blossom" Release (6e31ffc3, 2023−05−09) for windows).

Yeast Two-Hybrid Assays. The coding sequences of selected genes were inserted into the pGBKT7 and pGADT7 yeast two-hybrid vector system (Takara Bio USA, Inc.). Yeast strains Y187 and AH109 were transformed with the constructs using an LiAC method. Transformants were selected on SD/-Trp agar and SD/-Leu agar for pGBKT7 and pGADT7 constructs, respectively, at 28 °C for 5−7 days. The two strains were mated and grown on SD/-Trp/-Leu (Media Double Dropouts, DDO), SD/-Trp/-Leu/-His (Media Triple Dropouts, TDO), and SD/-Trp/-Leu/-His/-Ade (Media Quadruple Dropouts, QDO) at 28 °C for 5 days. Mating between the constructs with pGBKT7 and an empty pGADT7 vector and vice versa was used as the background control.

Analysis of T-DNA Insertion Mutants. gDNA was isolated by the CTAB method using 2−3 young leaves. Homozygous insertion lines for mutants were identified using a primer in Table S1. PCR was performed using 50 ng of gDNA in a 20 μL reaction volume containing 4 mM dNTPs, 30 mM $MgCl_2$, 0.5 μM for each primer, and 1 unit of *Taq* polymerase (Vivantis, Malaysia) using 35 cycles of 94 °C for 30 s, 60 °C for 45 s, and 72 °C for 1.15 min, with a final extension for 5 min. Individual plants identified as negative for the gene-specific amplification and positive for the left border amplification were considered homozygous line candidates. Seed progenies derived from the candidates were retested with PCR before being designated as homozygous lines.

Cell Wall Preparations. AIRs were prepared using a modified method from Pettolino et al.[27] Leaves of three-week-old plants were groud in liquid nitrogen, washed three times in 80% ethanol, absolute ethanol, acetone, and methanol, respectively, and then dried in an incubator at 55 °C. AIRs were extracted with 50 mM CDTA pH 7.0 at room temperature by shaking for 18 h before being filtered and collected using nylon mesh. The residue was subsequently extracted with 4 M NaOH containing 1% (w w^{-1}) $NaBH_4$ at room temperature with shaking for 18 h. The soluble fraction was collected by filtering using nylon mesh before being neutralized using glacial acetic acid. Both soluble fractions were dialyzed against distilled water at room temperature and then freeze-dried. The remaining cellulose residue was dried at 55 °C.

Cell Wall Composition Analysis. The CDTA and NaOH fractions were hydrolyzed with 2 M trifluoroacetic acid at 100 °C for 4 h before separation by high-performance anion-exchange chromatography on a Dionex Carbopac PA-10 column with pulsed amperometric detection as previously described.[28] Separated monosaccharides were quantified by external calibration using an equimolar mixture of nine monosaccharide standards (arabinose, fucose, rhamnose,

https://doi.org/10.1021/acsomega.4c00534
ACS Omega 2024, 9, 31438−31454

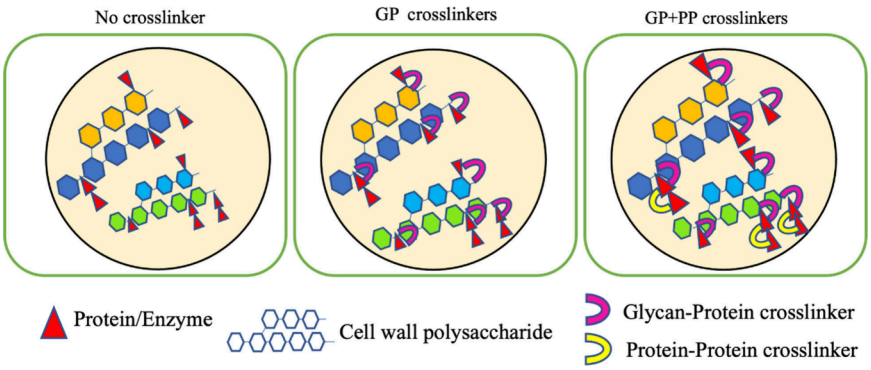

Figure 1. Schematic workflow of *in vivo* proximity cross-linking and immunoprecipitation of cell wall polysaccharides using *Arabidopsis* protoplasts. *Arabidopsis* protoplasts were prepared using young rosette leaves and subjected to nontreated or treated glycan−protein (GP) cross-linkers or glycan−protein and protein−protein (GP+PP) cross-linkers before immunoprecipitation using cell wall antibodies including LM15, LM28, LM21, and LM19. The illustration depicts cell wall polysaccharides that are being synthesized and interacted within the Golgi by various proteins or enzymes, which are then cross-linked to the polysaccharides by the treatment of GP cross-linkers. The treatment of GP+PP cross-linkers allows further proximity cross-linking of proteins to proteins cross-linked onto the polysaccharides.

xylose, glucose, galactose, mannose, glucuronic acid, and galacturonic acid). CDTA and NaOH fractions were calculated by combining the nine sugar contents. Cellulose content was quantified using Saeman hydrolysis[29] and Anthrone assay.[30]

Saccharification Analysis. Saccharification was performed following Gomez et al.[31] and Whitehead et al.[32] in 96-well-plate formats in a robotic platform (Tecan Evo200; Tecan Group Ltd.). Four milligrams of AIR samples were loaded into 96-deep-well plates, pretreated with 350 μL of 0.5 M NaOH solution at 90 °C for 30 min, washed for five times with 500 μL of 25 mM sodium acetate buffer pH 4.5, and then incubated with the enzyme cocktail at 50 °C for 8 h. The enzyme cocktail includes Celluclast (cellulose from *Trichoderma reesei*) and Novozyme 188 (Novozymes A/S, Bagavaerd, Denmark) at a ratio of 4:1 at an enzyme loading of 22.5 Filter Paper Unit (FPU) per gram of material. Biomass hydrolysates were analyzed for reducing sugar released using a modified MBTH method.[33] The experiment was performed using three biological replicates, each with four technical replicates. OD reads were converted to amounts of reducing sugars released in nanomoles using glucose standards.

RESULTS

Identification of Proteins Involved in Matrix Polysaccharide Biosynthesis by Proximity Cross-Linkers and Immunoprecipitation. To identify the biosynthetic machinery responsible for the synthesis of cell wall matrix polysaccharides, we employed a strategic approach involving *Arabidopsis* protoplasts and intracellular molecular cross-linkers, followed by immunoprecipitation using cell wall antibodies. The antibodies included LM15 recognizing XyGs,[34] LM28 recognizing GX,[35] LM21 recognizing GM,[36] and LM19 recognizing unesterified HGA.[37] Our approach is based on the concept that in vivo treatments of protoplast cells with cell-permeable GP cross-linkers would facilitate proximity cross-linking between cell wall matrix polysaccharides being assembled and cell wall biosynthetic enzymes or other related proteins actively functioning in the Golgi network through to secretory vesicles. Furthermore, PP cross-linkers can be added to further extend the network of targets to other associated proteins. Once cross-linked, different matrix polysaccharides, along with their cross-linked proteins, can be isolated through immunoprecipitation using cell wall specific antibodies, followed by protein identification using LC/MS/MS. For this instance, we selectively acquired cell-permeable cross-linkers based on the cross-linker selection tool (Thermo Fisher Scientific). There are five and six cell-permeable reagents for *in vivo* cross-linking of GP and PP interactions, respectively. Notably, BMOE (bismaleimidoethane) was chosen as a PP cross-linker, having been used for *in vivo* cross-linking experiments in various organisms including *E. coli*,[38,39] *Bacillus subtilis*,[40] yeasts,[41] and human endothelial cells and platelets.[42] It is important to note that while GP cross-linkers have been used for *in vitro* cross-linking assays[43−45] their *in vivo* cross-linking potential has remained unexplored. Here, we selected four cell-permeable GP cross-linkers, namely, KMUH (*N*-κ-maleimidoundecanoic acid hydrazide), EMCH (*N*-ε-maleimidocaproic acid hydrazide), BMPH (*N*-β-maleimidopropionic acid hydrazide), MPBH (4-(4-*N*-maleimidophenyl)butyric acid hydrazide), and BMOE (PP cross-linker), for *in vivo* cross-linking experiments. We used *Arabidopsis* protoplasts to avoid any interference from extracellular cell wall epitopes during the immunoprecipitation using cell wall antibodies. Therefore, only cell wall epitopes along with their cross-linked proteins that reside within the cell can be specifically targeted. The experimental workflow is illustrated in Figure 1. Protoplasts were isolated from *Arabidopsis* leaves using the Tape-*Arabidopsis* Sandwich method.[22] Three treatments of *Arabidopsis* protoplasts were performed: (a) no cross-linker treatment (aimed to isolate proteins tightly associated with cell wall polymers); (b) GP cross-linkers (a mixture of KMUH, EMCH, BMPH, and MPBH at 1 mM each) targeting proteins directly interacting with glycans; and (c) combined GP+PP cross-linkers (the GP mixture and 1 mM BMOE) targeting those associated with proteins linked to glycans. The protoplasts were treated with the cross-linkers by incubation at 25 °C for 2 h before total protein extraction and immunoprecipitation.

Peptide analysis by LC-MS/MS from the four antibodies, each with the three treatments, resulted in a total of 218 peptide fragments ranging from 8 to 39 amino acids. BLASTP analysis of these peptides led to the identification of 110 protein identities (IDs) based on the *Arabidopsis* genome. The total peptide reads and protein IDs for each antibody and treatment are presented in Table S2. The reliability of our protein identification was supported by the confirmation of

https://doi.org/10.1021/acsomega.4c00534
ACS Omega 2024, 9, 31438−31454

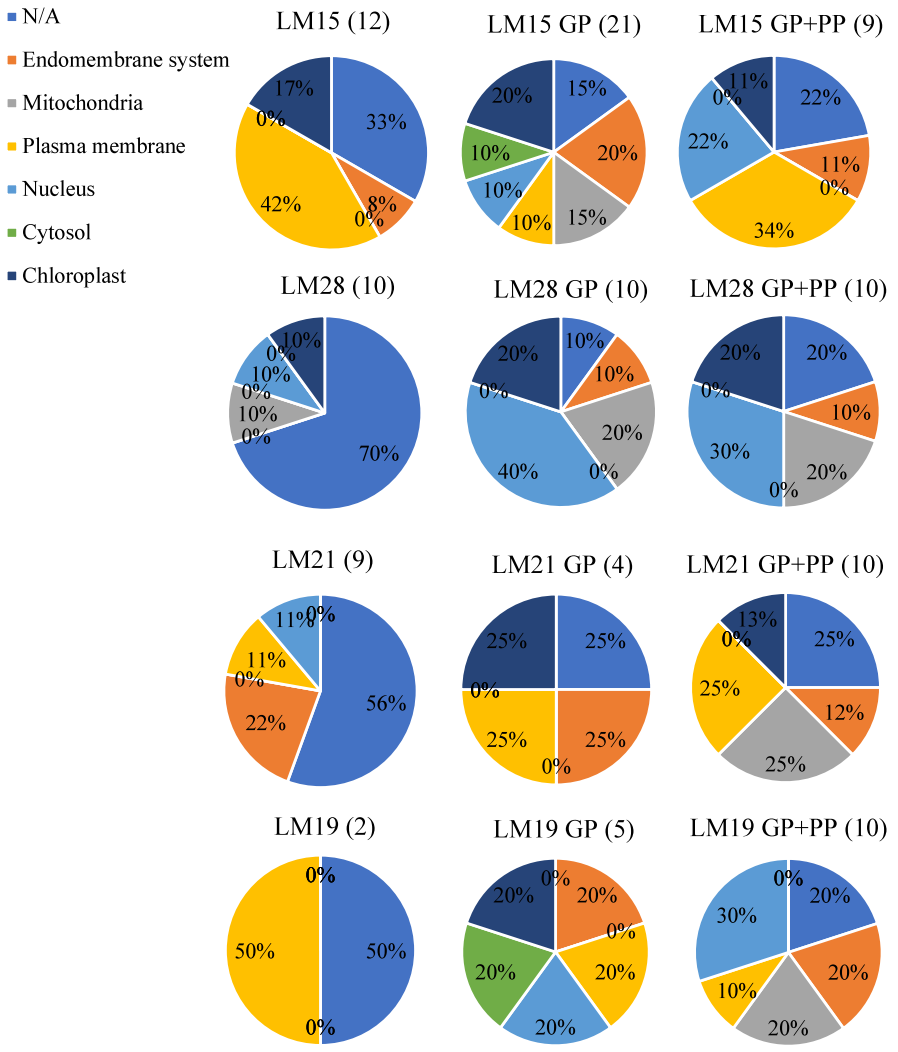

Figure 2. Proteomic analysis of immunoprecipitated products using cell wall antibodies. Identified proteins were classified based on annotated subcellular localizations. The number of proteins identified for each antibody and treatment are presented. Diagrams show percentages of proteins for each localization compartment.

several protein IDs through alignments with an average of two fragments (maximum of 11 fragments) located within each protein. In total, the numbers of proteins IDs identified for no cross-linkers, GP cross-linkers, and GP+PP cross-linkers for each antibody are as follows: 12, 21, and 9 IDs for LM15, 10, 10, and 10 IDs for LM28, 9, 4, and 10 IDs for LM21 and 2, 5, and 10 IDs for LM19. We classified these proteins based on their subcellular localizations using gene annotations and experimental reports (Figure 2 and Table S2). The identified protein originated from various cellular compartments, including endomembrane systems, mitochondria, plasma membrane, nucleus, cytoplasm, and chloroplast. However, a substantial number of these proteins lacked specific information regarding localization. Since our focus was on identifying proteins involved in cell wall matrix polysaccharides, we present protein IDs that were either reported or predicted to be localized in the Golgi, ER, endomembrane, plasma membrane, and those without localization data (Table 1). Accordingly, there are 26, 14, 17, and 8 protein IDs for LM15, LM28, LM21, and LM19, respectively. Notably, two proteins, At1g58602 from LM15 and At1g13210 from LM19, were identified in both GP and GP+PP treatments, suggesting their interaction with their respective cell wall polymers and affirming the reliability of our method.

We identified several glycosyltransferases directly involved in synthesizing cell wall polysaccharides in the Golgi, including galactomannan galactosyltransferase (MBGT1, At4g13990), putative GT14 Arabinogalactan synthesis (At3g03690), callose synthase (GSL4, At3g14570) from LM15 (GP), putative galacturonosyltransferase 2 (GAUT2, At2g46480) from LM28 (GP), and putative pectin acetyltransferase (TBL42, At1g78710) from LM21 (GP+PP). We observed other proteins involved in matrix polysaccharide biosynthesis and cell wall modification such as the UDP-xylose transporter (At2g30460) from LM15, beta-glucosidase 6 (At3g60130) from LM28, and beta-xylosidase (At5g09730) from LM21. Furthermore, we found the Rho GTPase activation protein (PHGAP1, At5g12150) from LM15 GP+PP that has been shown to be involved in cell wall patterning and a formation of pavement cell shape through an interaction with Rho-related GTPases. These findings demonstrate the effectiveness of our method, involving molecular cross-linkers, protoplasts, and immunoprecipitation using cell wall antibodies in isolating and identifying proteins actively involved in the process of matrix polysaccharide biosynthesis within the plant cell.

https://doi.org/10.1021/acsomega.4c00534
ACS Omega 2024, 9, 31438−31454

Table 1. Protein Identification Obtained from Immunoprecipitation of Leaf Protoplasts Using Cell Wall Antibodies[a]

Protein	Annotation	Peptide length	Localization	DeepAraPPI/ ATMAD	Ref
	LM15 GP				
At1g58602	LRR and NB-ARC domain-containing disease resistance protein	26	-	Y/Y	
At4g13990	beta-GGM galactosyltransferase (beta-MBGT1)	26	Golgi	N/N	46
At1g78000	Sulfate transporter 1; 2	36	PM	N/Y	47, 48
At4g14880	O-acetylserine (thiol) lyase (OAS-TL) isoform A1	9	-	N/Y	49, 50
At3g22460	O-acetylserine (thiol) lyase (OAS-TL) isoform A2	34	-	Y/Y	49, 50
At1g19610	*Arabidopsis* defensin-like protein	12	ES	N/N	
At5g48620	Resistance protein Ler3	9	PM	N/N	
At3g03690	Core-2/I-branching beta-1,6-N-acetylglucosaminyltransferase family protein (GT14 family)	19	ES	N/N	
At3g14570	Glucan synthase-like protein (GSL4)	13	-	N/N	51
At2g35130	Tetratricopeptide repeat (TPR)-like superfamily protein	22	ES	N/N	52
	LM15 GP+PP				
At1g58602	LRR and NB-ARC domain-containing disease resistance protein	18	-	Y/Y	
At2g05520	Glycine-rich protein 3 short isoform	9	ES	Y/Y	53
At5g43350	Phosphate transporter 1	19	PM	N/Y	54
At1g18890	Calcium-dependent protein kinase 1	26	PM	Y/N	55
At4g15500	UDP-Glycosyltransferase superfamily protein, hydroxycinnamate glucosyltransferase (UGT84A4)	30	-	N/N	56
At5g12150	Rho GTPase activation protein (PHGAP1)	33	PM	N/N	57
	LM15				
At1g07950	Mediator of RNA polymerase II transcription subunit 22b	29	-	Y/N	
At2g39880	Transcription factor MYB25	24	-	N/N	58
At5g65270	Ras-related protein RABA4a	22	PM	Y/N	
At1g76850	Exocyst complex component SEC5A	28	PM	Y/Y	
At2g30460	UDP-xylose transporter 2	31	ES	N/N	59
At3g07040	Disease resistance protein RPM1	12	PM	Y/Y	
At4g15215	ABC transporter G family member 41	23	Membrane	Y/Y	
At3g29580	MATH domain and coiled-coil domain-containing protein	28	-	N/N	
At3g03330	Rossmann-fold NAD(P)-binding domain-containing protein	14	ER, PM	N/Y	
At5g45720	AAA-type ATPase family protein	23	-	N/N	
	LM28 GP				
At4g06598	BZIP transcription factor-like protein	15	-	N/N	
At5g44920	Toll-Interleukin-Resistance (TIR) domain family protein	36	ER	N/Y	
At2g46480	Galacturonosyltransferase 2 (GAUT2)	22	Golgi	N/N	60
At2g43700	Concanavalin A-like lectin protein kinase family protein	35	ES	Y/Y	
	LM28 GP+PP				
At1g78500	Terpenoid cyclases family protein	21	-	N/N	
At5g22290	NAC domain containing protein 89	11	ER, nucleus	Y/Y	61
At5g38396	F-box/RNI-like superfamily protein	31	-	N/N	
	LM28				
At4g28400	Probable protein phosphatase 2C 58	25	-	N/N	
At3g16440	Jacalin-related lectin 32	24	-	Y/Y	
At1g71170	Probable 3-hydroxyisobutyrate dehydrogenase-like 2	28	-	N/N	
At3g60740	Tubulin-folding cofactor D	30	-	N/N	
At5g02980	Putative F-box/kelch-repeat protein	31	-	N/N	
At3g58220	MATH domain and coiled-coil domain-containing protein	29	-	N/N	
At3g60130	Beta-glucosidase 16	24	-	Y/Y	
	LM21 GP				
At4g25350	EXS (ERD1/XPR1/SYG1) family protein	31	-	N/N	62
At4g08560	Pumilio-family RNA binding repeat (PUF)	36	ES	N/N	
At1g03750	Chromatin modification-related protein EAF1	34	PM	N/N	
	LM21 GP+PP				
At1g22882	Galactose-binding protein	21	Nucleus, ER	N/Y	
At1g55020	Lipoxygenase 1	32	-	N/Y	
At3g56480	Myosin heavy chain-related	20	PM	N/N	
At1g78710	Trichome birefringence-like 42 (TBL42)	29	ES	N/N	
At3g02260	Auxin transport protein BIG	21	PM	N/Y	
At4g25520	Lim domain-binding protein	37	-	N/Y	

https://doi.org/10.1021/acsomega.4c00534
ACS Omega 2024, 9, 31438−31454

Table 1. continued

Protein	Annotation	Peptide length	Localization	DeepAraPPI/ ATMAD	Ref
	LM21				
At1g55325	Mediator of RNA polymerase II transcription subunit 13	34	-	Y/Y	
At5g09730	Beta-D-xylosidase 3	33	ES	N/N	
At2g02950	Phytochrome kinase substrate 1	25	-	N/Y	
At4g02050	Sugar transport protein 7	32	PM	Y/N	
At3g60240	Eukaryotic translation initiation factor 4G	21	-	N/N	
At2g45880	Beta-amylase 7	34	-	Y/N	
At1g74900	Pentatricopeptide repeat-containing protein	27	-	N/N	
At1g30710	Berberine bridge enzyme-like 14	29	ES	N/N	
	LM19 GP				
At1g13210	Probable phospholipid-transporting ATPase 11	13	PM	N/N	
At1g58250	Golgi-body localization protein domain; RNA pol II promoter Fmp27 protein domain	24	Golgi	N/N	63
	LM19 GP+PP				
At1g17580	Myosin 1	26	-	Y/Y	64
At4g32150	Vesicle-associated membrane protein 711	36	VM	Y/Y	65, 66
At5g13740	Zinc induced facilitator 1	37	VM	N/N	67
At1g13210	Probable phospholipid-transporting ATPase 11	13	PM	N/N	
	LM19				
At1g20925	Protein PIN-LIKES 1	28	Membrane	N/N	
At3g21130	Putative F-box protein	11	-	Y/Y	

[a]The longest peptide chains obtained from LC-MS/MS for each protein. Protein localization data were obtained from the literature and ThaleMine database. Protein interaction data were obtained from the DeepAraPPI and ATMAD database. GP: glycan−protein crosslinker, PP: protein−protein crosslinker. Plasma membrane: PM, endomembrane system: ES, vacuole membrane: VM.

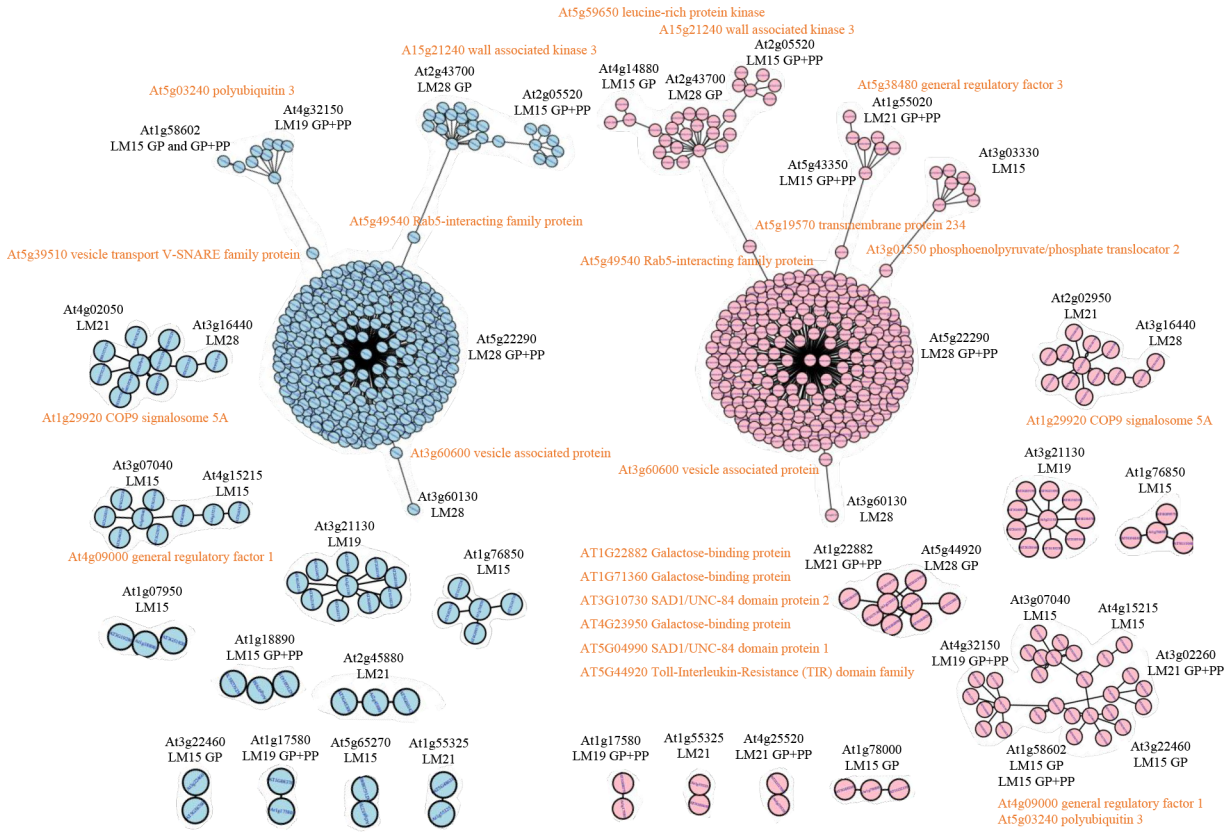

Figure 3. Protein interaction networks based on DeepAraPPI (in blue) and AtMAD (in pink). Each cluster represents a protein ID (*Arabidopsis* accession and its pull down condition) as a center connected to a number of interacting proteins, as found in each database. The networks were built based on common *Arabidopsis* gene accessions found for each protein ID. Interacting proteins known to be associated with the cell wall and those that connect between clusters are indicated.

In addition, the identified protein IDs also include proteins that are typically targeted to the cell walls or involved in cellular machinery for vesicle trafficking. Notably, disease resistance protein RPM1 (At3g07040) from LM15, resistant

https://doi.org/10.1021/acsomega.4c00534
ACS Omega 2024, 9, 31438−31454

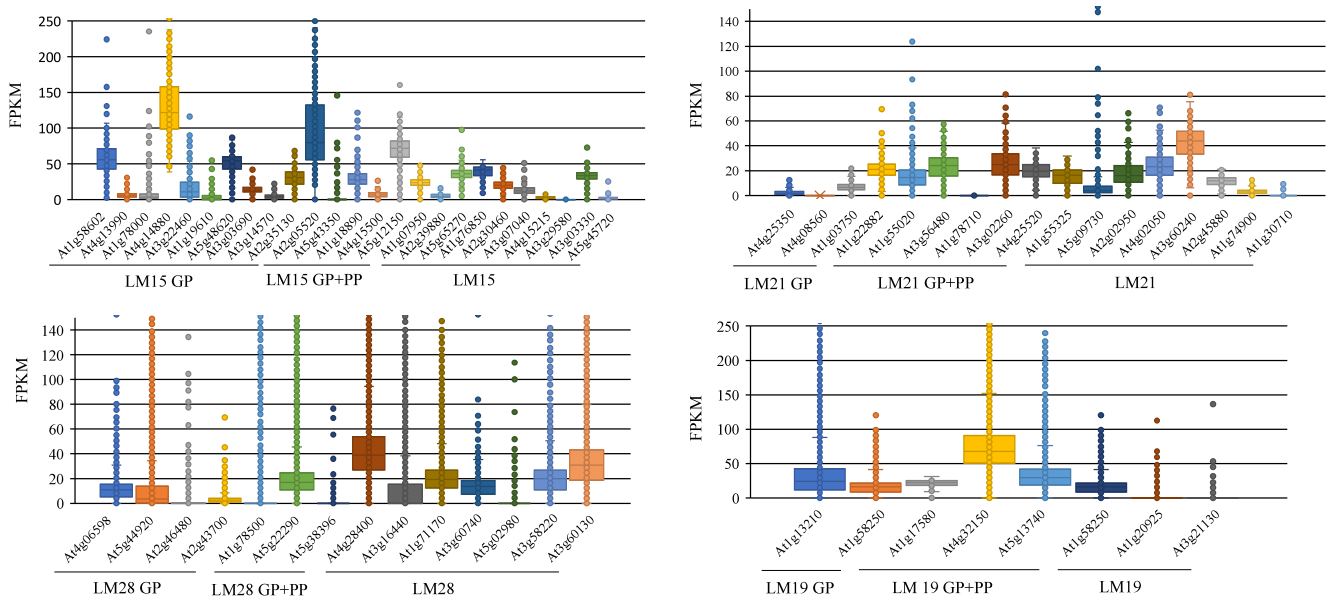

Figure 4. Gene expression levels of the protein IDs from four antibodies in *Arabidopsis* leaf tissues. Data was obtained from the *Arabidopsis* RNA-seq database.

proteins (At5g48620) from LM15 (GP), *Arabidopsis* defensin-like protein (At1g19610) from LM15 (GP), and glycine-rich protein 3 (At2g05520) from LM15 (GP+PP) were found in the cell wall and are known to play roles in conferring resistance to various pathogens and pests. Furthermore, exocyst complex proteins (At1g76850) from LM15, Golgi localization protein domain (At1g58250) from LM19 (GP), and vesicle-associated membrane protein 711 (At4g32150) from LM19 (GP+PP) were identified, indicating their association with matrix polysaccharides and their involvement in Golgi and vesicle protein components. Interestingly, there are some proteins that have never been reported to be associated with the plant cell wall, such as the kinesin motor family protein, sulfate transporter 1, and tetratricopeptide repeat. This result suggests that these proteins may have a potential association with the synthesis of matrix polysaccharides, representing novel candidates for further investigation. Taken together, our results have identified proteins that are directly or indirectly involved in cell wall matrix polysaccharides, from their synthesis to delivery. The use of cross-linkers has shown their ability to capture these associations, providing insights for further detailed functional studies.

Identification of Proteins Based on Protein Interactions. To identify the relationship of these proteins to the plant cell wall, we performed searches for *Arabidopsis* protein interactions using DeepAraPPI (based on deep learning-assisted prediction)[23] and AtMAD (based on experimental data such as FRET, yeast-2-hybrid, coimmunoprecipitation, and affinity capture-MS)[24] databases. Protein/gene IDs that matched the protein interaction databases are indicated in Table 1. Out of the 63 IDs, 19 and 24 were found in DeepAraPPI and AtMAD databases, respectively. Figure 3 shows a summary of the protein interaction networks from the two databases (the full lists of interacting proteins for each ID are presented in Files S1 and S2). The protein interaction networks obtained from both databases showed considerable similarity. Notably, a large network was observed for At5g22290 (NAC domain containing protein 89; LM28 GP +PP) in connection with five or seven IDs (depending on the databases) obtained from the four antibodies and with a large number of proteins (314 and 238 proteins for DeepAraPPI and AtMAD, respectively). This suggests that At5g22290 may have extensive interactions with other proteins related to cell wall biosynthesis. Among these interactions, we found connections to cellulose synthase-like proteins (CSLs), arabinogalactan proteins (AGPs), glycosylhydrolase (GHs), pectin methylesterase inhibitors (PMEIs), pectin lyase-like proteins, nucleotide sugar transporters, and other cell-wall-related proteins. Additionally, At5g22290 indirectly interacts with other proteins, including At2g43700 (Concanavalin A-like lectin protein kinase family protein) from LM28 GP, At4g32150 (vesicle-associated membrane protein 711) from LM19 GP+PP, and At3g60130 (beta-glucosidase 16) from LM28, through membrane and vesicle trafficking proteins, including the Rab5-interacting family protein, V-SNARE family protein, and vesicle-associated protein. The cross interactions among the proteins identified with the four antibodies suggest proximity networks of the proteins associated with the four polysaccharides from both hemicelluloses and pectins. This observation validates our method for *in vivo* proximity cross-linking immunoprecipitation.

Interestingly, we found a branch in the network of At2g43700 that connects to At2g05520 (glycine-rich protein 3 short isoform) via wall associated kinase 3 and to At4g14880 (O-acetylserine (thiol) lyase) via a leucine-rich repeat protein kinase family protein. At2g05520 itself was also found to interact with wall-associated kinases. This observation may indicate a potential signaling network linking membrane/vesicle systems to cell wall polysaccharides.

While smaller networks with a few or single IDs were also observed, they did not show further associations with cell-wall-related proteins. Alternatively, we found networks for At4g02050−At3g16440 and At3g07040−At4g15215 from DeepAraPPI and AT2g02950−At3g16440 and the network of the five IDs (At4g32150, At3g07040, At4g15215, At3g02260, At3g22460, and At1g58602) from AtMAD involving the protein degradation pathway, such as COP9 signalosome 5A, polyubiquitin 3, and, perhaps, general

https://doi.org/10.1021/acsomega.4c00534
ACS Omega 2024, 9, 31438−31454

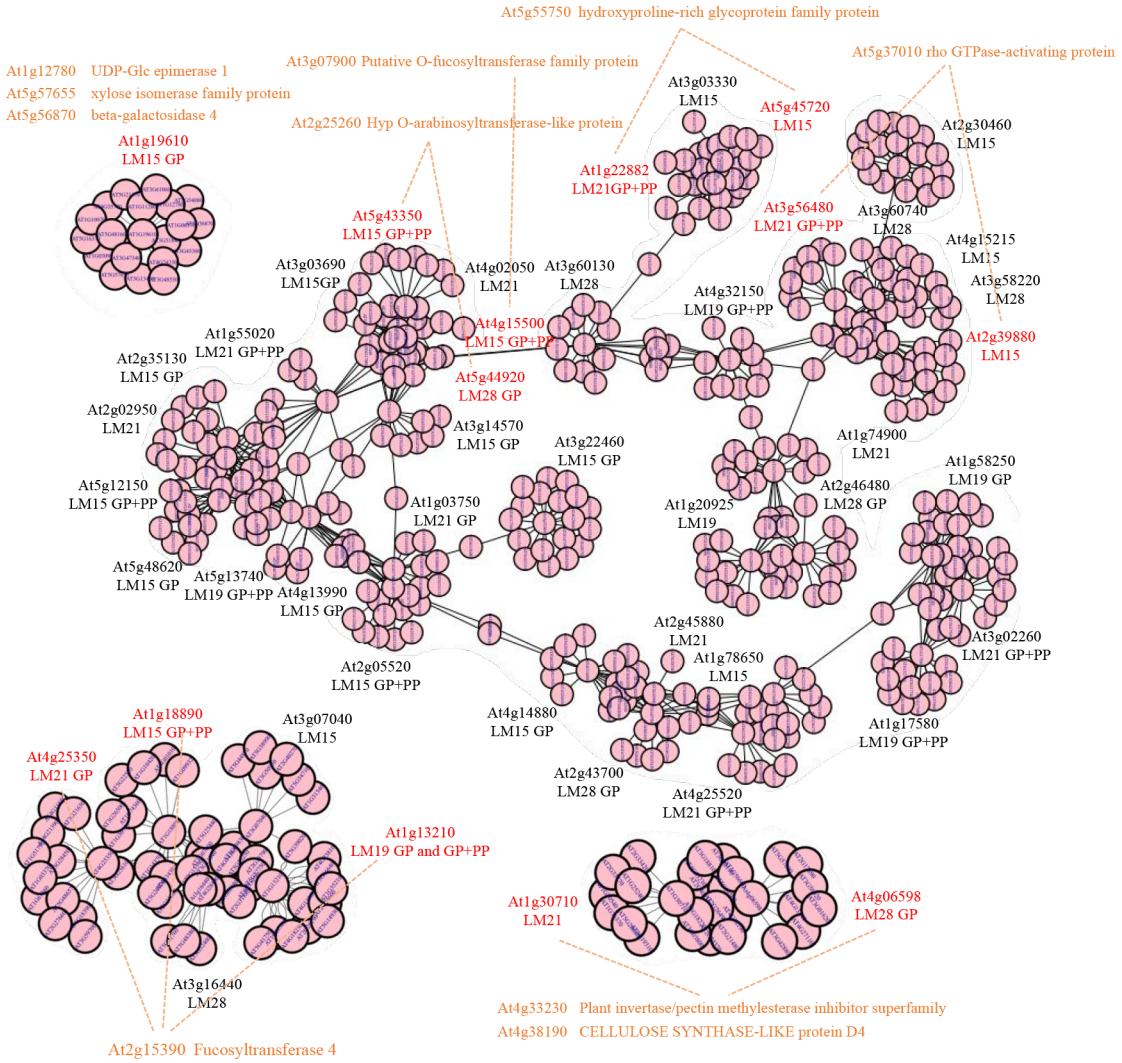

Figure 5. Coexpression network based on the *Arabidopsis* RNA-seq database. Only protein IDs with coexpressors related to cell walls (in red) and those IDs that are connected through the networks are presented. Protein IDs with their pulldown conditions are presented for each cluster. Coexpressors related to cell wall processes are presented in orange text with connected lines to their corresponding IDs.

regulatory factor 1. Furthermore, the At1g22882−At5g44920 network from AtMAD forms a network among galactose binding protein/SAD1/UNC-84 domain protein/Toll-Interleukin-Resistance (TIR) domain family protein, and this may play a role in the TLR signaling pathway. Although further investigation is required to confirm these interactions and their functional relevance, our results indicate that the molecular cross-linkers, cell wall antibodies, and the immunoprecipitation method employed in this study have identified putative proteins associated with matrix polysaccharide biosynthesis occurring within plant cells.

To further validate the identified proteins and their interactions, we sought to perform yeast-two-hybrid assays. However, directly testing glycan−protein interactions was challenging, and we were unable to verify this aspect. Nevertheless, for the protein IDs identified through GP+PP cross-linkers, which were based on protein−protein interactions, we conducted yeast-two-hybrid assays to assess interaction within each antibody group (see Table S3 for the list). After careful assay with negative controls, we did not observe any direct interactions among the proteins. Instead, we found evidence of homomultimeric proteins (indicated in Table S3).

Identification of Proteins Based on Gene Expression and Coexpression Analysis. To validate the presence and relevance of the identified protein IDs in leaf tissues, we examined the expression levels of genes encoding these proteins using data obtained from the *Arabidopsis* RNA-seq database.[25] Figure 4 shows that the genes encoding the protein IDs are generally expressed in the leaf, with some of the IDs showing very low expression levels. Among them, At4g14880 (LM15 GP) and At2g05520 (LM15 GP+PP) exhibited the highest expression levels. The RNA-Seq data confirm that these genes are expressed in leaf tissues and are functional in the protoplasts.

Next, we examined coexpression analysis of the genes encoding the protein IDs from the *Arabidopsis* RNA-seq Database. Due to the large number of coexpressors for each ID, we selected the top 20 candidates and examined their functional annotations (see the lists of coexpression for each gene ID in File S3). Figure 5 presents the coexpression networks of the top candidates, focusing on those that are associated with cell wall-related genes. Out of the 63 gene IDs,

https://doi.org/10.1021/acsomega.4c00534
ACS Omega 2024, 9, 31438−31454

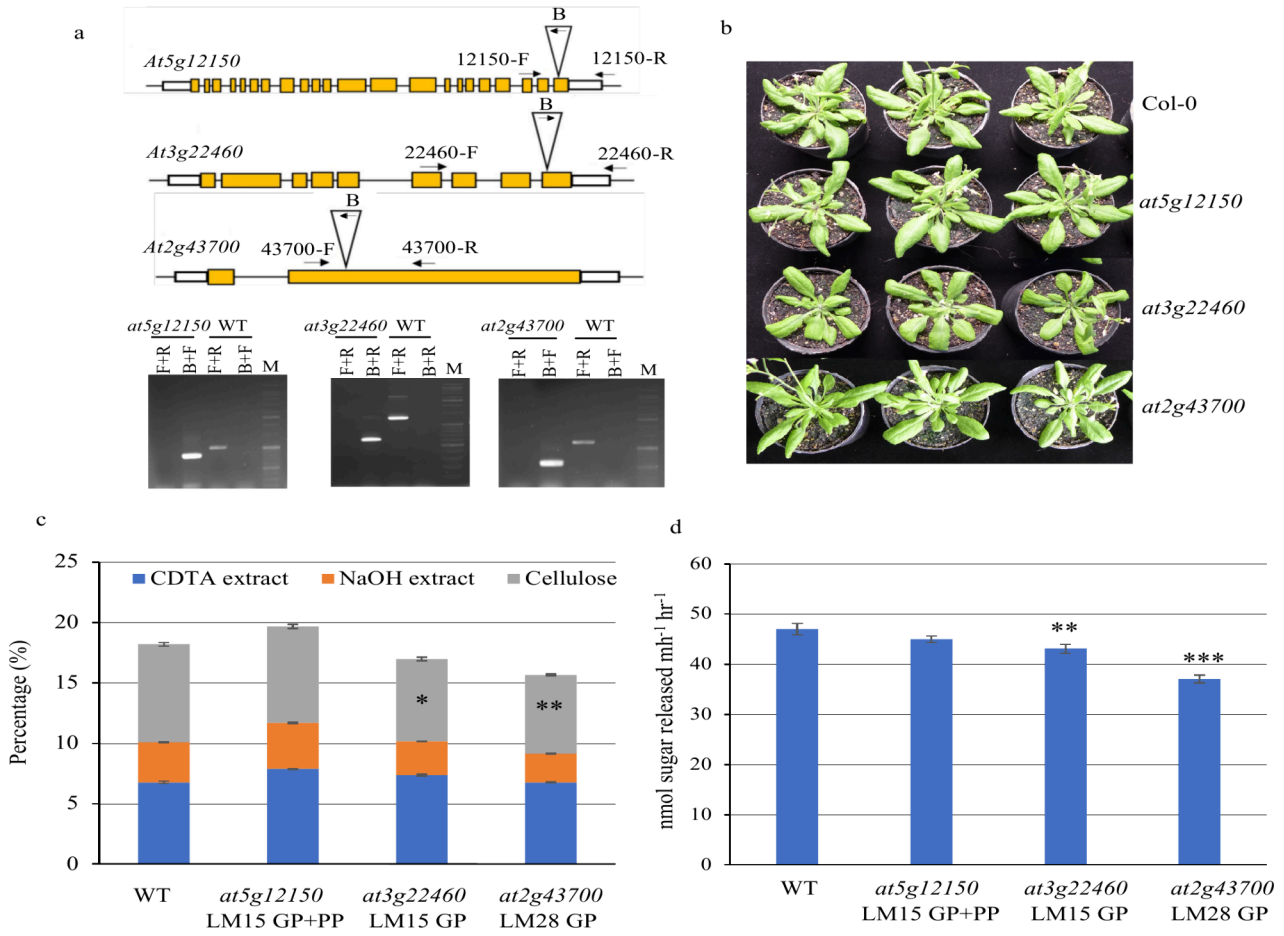

Figure 6. Characterization of T-DNA insertion mutants on proteins identified using cross-linking and immunoprecipitation. (a) T-DNA insertion positions are indicated within the gene structures. Arrows indicate the direction of PCR primers for genotyping including forward (F) and reverse (R) primers and the border (B) primer. The lower panel shows identification of homozygous lines using flanking and border primer combinations. M indicates DNA ladder (see full-length gels in Figure S1). (b) Four-week old plants of three mutants at an early bolting stage grown alongside WT plants. (c) Mass yield of CDTA extract, NaOH extract, and cellulose residue of AIRs obtained from leaves. Data were obtained from three biological replicates presented with SE (n = 3). (d) Saccharification analysis of the three mutants presented as reducing sugars released by enzymatic hydrolysis of pretreated AIR samples (three biological replicates and each with four technical replicates) (n = 3). Asterisks indicate significant differences from WT using student's t test (*$P \leq 0.05$, **$P \leq 0.01$, ***$P \leq 0.001$).

13 were found to have coexpression with cell wall-associated genes. Interestingly, we observed a large coexpression network comprising seven genes that are coexpressed with cell wall-associated genes and 31 genes without coexpression with cell wall genes. This network is associated with cell wall genes through a hydroxyproline-rich glycoprotein (HRGP), HRGP O-arabinosyltransferase, O-fucosyltransferase, and rho GTPase-activating protein genes. Additionally, we found that genes At1g19610 had coexpressors that interacted with cell wall-associated genes such as UDP-Glu epimerase, xylose isomerase, and beta-galactosidase 4. At1g30710 and At4g06598 are coexpressed with a putative PMEI (At4g33230) and CSLD4 (At4g38190). Furthermore, we identified a coexpression network involving five genes (At4g25350, At1g18890, At3g07040, At1g13210, and At3g16440) that connected to At2g15390 (arabinogalactan protein fucosyltransferase 4, AtFUT4), suggesting the potential function of these genes with the biosynthesis of cell wall components. These coexpression networks provide evidence that these proteins may indeed be associated with plant cell walls, despite not having been previously reported in this context. The expression analysis and coexpression networks provide further support for the involvement of the proteins identified in leaf cell wall biosynthesis.

Characterization of Cell Wall Associated Proteins Using *Arabidopsis* T-DNA Insertion Mutants. To validate our method, we employed reverse genetics to target three of the proteins identified. At5g12150 (LM15 GP+PP) was chosen as Rho GTPase activation proteins (PHGAP1 and PHGAP2), and Rho GTPase have been shown to be involved in cell wall patterning and directing the formation of cell wall pits in metaxylem vessel cells.[68−70] At3g22460 (LM15 GP), an O-acetylserine (thiol) lyase, which plays a role in the final step in the cysteine biosynthetic pathway, has never been shown to be related to the plant cell wall. At2g43700 (LM28 GP), a Concanavalin A-like lectin protein kinase family protein, was selected based on its protein interaction data, suggesting associations with other cell wall components, including Wall Associated Kinases, via the At5g22290 protein. T-DNA insertion mutants for these genes were obtained, and homozygous lines were identified through PCR genotyping (Figure 6a). No visible alterations were observed in these mutants, except for slightly slower growth in the *at3g22460* mutant compared to WT. However, when we performed cell

https://doi.org/10.1021/acsomega.4c00534
ACS Omega 2024, 9, 31438−31454

wall compositional analysis on these mutants, we found significant reductions ($P < 0.05$) in cellulose content in the *at3g22460* and *at2g43700* mutants. Subsequently, saccharification analysis using Alcohol Insoluble Residue (AIR) from leaves revealed that both mutants had significantly less saccharification potential compared to the WT ($P < 0.01$). This reduction in saccharification potential is likely a consequence of the reduced cellulose content in the cell walls of these mutants. Furthermore, the monosaccharide composition of the CDTA extracts of both mutants showed reductions in Xyl and GluA, along with increases in GalA, relative to the WT (Table 2). Likewise, substantial changes in all monosaccharides, except Glu and Man, were found in the NaOH extract of both mutants. However, no alterations in cell wall and monosaccharide compositions were observed in the *at5g12150* mutant. Since At3g22460 and At2g43700 proteins were identified through LM15 and LM28 with GP cross-linkers, respectively, it is likely that these proteins were present in close proximity to XyG and GX, respectively, during the biosynthesis of these polysaccharides. Indeed, the reductions of Xyl and GluA in CDTA and NaOH extracts reflect the potential relationships of these proteins to XyG and GX, while changes in various sugar compositions in the NaOH extract suggest the impact of these proteins on other polysaccharides. These results indicate that T-DNA insertions in At3g22460 and At2g43700 lead to changes in the cell wall, resulting in reduced cellulose content and altered matrix polysaccharide compositions. The changes in the cell wall of these mutants support their potential roles in cell wall biosynthesis.

DISCUSSION

We present a new approach for identifying proteins involved in cell wall matrix polysaccharide biosynthesis by utilizing *in vivo* proximity cross-linking and immunoprecipitation in *Arabidopsis* protoplasts. We used protoplast to ensure the exclusion of immunoprecipitation of epitopes in the cell wall. This approach allowed us to capture proteins actively associated with cell wall polymers: proteins directly interacting with glycan and those associated with protein linked to glycans. We focused on cell wall-related proteins by narrowing down the IDs to those predicted or reported to be localized in the Golgi, ER, plasma membrane, and those without specific localization data. We found several glycosyltransferases directly involved in cell wall polysaccharide synthesis, along with other proteins involved in cell wall modification and those typically targeted to cell walls or involved in vesicle trafficking. Protein interaction networks showed interactions between various proteins, including those related to cell wall-associated proteins and membrane/vesicle trafficking proteins. Gene expression and coexpression analysis supported the presence and relevance of the proteins identified in leaf tissues. Reverse genetic studies using T-DNA insertion mutants of selected proteins revealed changes in cell wall composition, monosaccharide composition and saccharification potential supporting their potential roles related to cell wall biosynthesis. Further investigations are necessary to unravel the precise functions of these proteins in the complex process of cell wall biosynthesis.

Chemical cross-linkers are compounds designed to covalently bind to specific functional groups on molecules, facilitating their physical interaction and stabilization. In our study, we employed four different chemical cross-linkers, KMUH, EMCH, BMPH, and MPBH, to specifically cross-link

Table 2. Cell Wall Monosaccharide Composition Analysis of CDTA and NaOH Extracts of Leave Samples from the Selected Mutants, Expressed in μg of Each Monosaccharide per mg of Biomass[a]

	Fuc	Ara	Rha	Gal	Glu	Xyl	Man	GalA	GluA
CDTA extract									
WT	1.40 ± 0.04	6.94 ± 0.08	6.41 ± 0.11	9.05 ± 0.06	14.96 ± 1.2	4.10 ± 0.06	1.24 ± 0.06	22.91 ± 1.54	0.71 ± 0.02
at5g12150	1.43 ± 0.15	5.77 ± 0.07	6.68 ± 0.25	8.75 ± 0.34	18.64 ± 2.7	3.53 ± 0.04	1.53 ± 0.28	31.54 ± 3.87	1.03 ± 0.05
at3g22460	1.19 ± 0.21	5.21 ± 0.35	5.22 ± 0.36	7.53 ± 0.7	13.26 ± 2.78	2.33 ± 0.28*	1.05 ± 0.24	37.35 ± 3.46	0.61 ± 0.03*
at2g43700	1.43 ± 0.09	5.32 ± 0.19	5.48 ± 0.11	6.97 ± 0.03	7.94 ± 1.65	2.58 ± 0.11*	0.85 ± 0.08	36.58 ± 1.85*	0.54 ± 0.04*
NaOH extract									
WT	1.61 ± 0.1	3.66 ± 0.21	1.60 ± 0.18	6.22 ± 0.31	13.00 ± 4.3	5.92 ± 0.13	1.85 ± 0.37	3.50 ± 0.16	0.83 ± 0.07
at5g12150	1.87 ± 0.06*	3.69 ± 0.3	1.60 ± 0.08	7.04 ± 1	10.88 ± 1.78	6.38 ± 0.89	2.31 ± 0.41	3.70 ± 0.27	0.72 ± 0.13
at3g22460	1.23 ± 0.02*	2.27 ± 0.04**	0.96 ± 0.14**	5.49 ± 0.12*	9.61 ± 0.73	4.26 ± 0.31**	1.48 ± 0.04	2.22 ± 0.04**	0.42 ± 0.02**
at2g43700	1.24 ± 0.06*	2.20 ± 0.35**	0.92 ± 0.05*	4.97 ± 0.81	7.32 ± 1.56	3.54 ± 0.62*	1.34 ± 0.25	1.96 ± 0.13***	0.41 ± 0.01**

[a]Data were obtained from three biological replicates presented with SE ($n = 3$). Asterisks indicate significant differences from WT using student's t-test (*$P \leq 0.05$, **$P \leq 0.01$, ***$P \leq 0.001$).

https://doi.org/10.1021/acsomega.4c00534
ACS Omega 2024, 9, 31438−31454

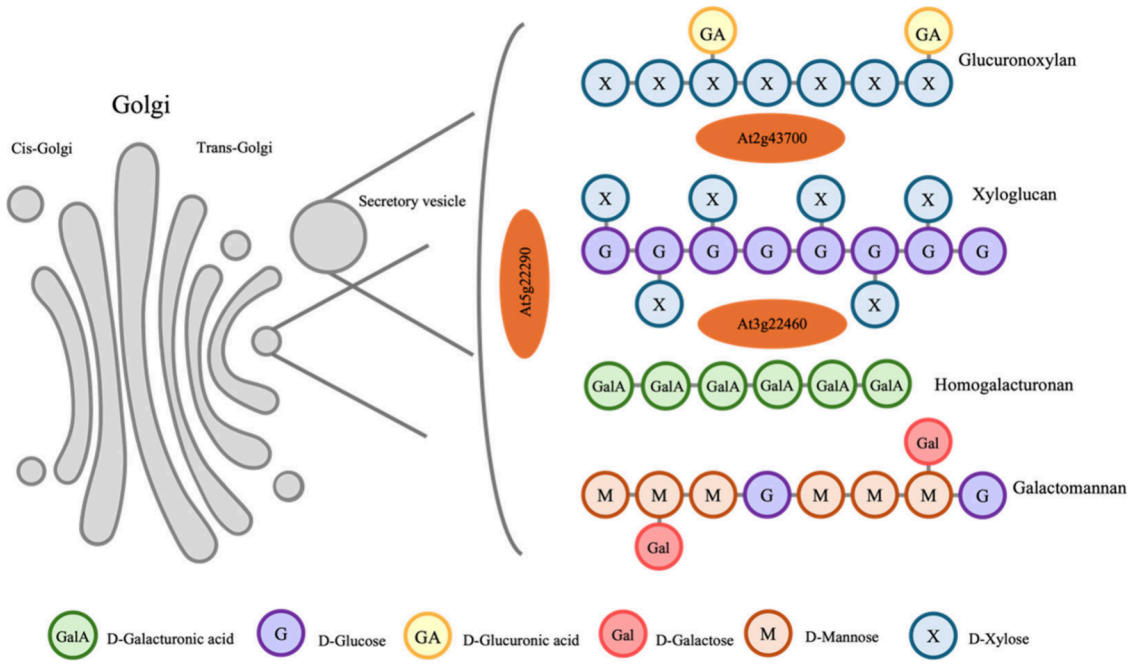

Figure 7. Schematic representation of the localization of matrix cell wall polysaccharide biosynthesis within the Golgi apparatus. Matrix polysaccharides are represented within the Golgi network. Specifically, matrix polysaccharides are synthesized entirely within the trans-Golgi and subsequently transported to the extracellular space via secretory vesicles. Our study shows the presence of matrix polysaccharides for both hemicelluloses and pectins within the Golgi and secretory vesicles, indicating their close proximity and polysaccharide−protein interacting networks. We identified At5g22290 as a candidate hub protein interacting with other cell wall-related proteins involved in XyG, GX, and GM biosynthesis. Furthermore, At2g43700 was identified as a protein interacting with GX and linked to other proteins involved with XyG, while At3g22460 interacts with XyG and is linked to other proteins involved with GM and HGA.

glycans or carbohydrates to proteins. These are hydrazide cross-linkers with a maleimide group that reacts with free thiol groups (-SH) on cysteine residues in proteins, enabling the preservation of glycan-protein interactions in their native state as they form stable covalent bonds. This approach has been previously used for studying glycan-protein interactions and their roles in various cellular processes.[71] Additionally, our method employed BMOE as a chemical cross-linker to specifically cross-link proteins to proteins through two maleimide groups that can react with free thiol groups on cysteine residues in different proteins, forming covalent bonds between them. While no cross-linker treatments represent proteins that directly and tightly bind to matrix polysaccharides without the help from cross-linkers, the use of chemical cross-linkers in our experiment serves as a valuable tool to preserve and stabilize glycan-protein interactions and protein−protein interactions.

We observed that the protein IDs identified through LC-MS/MS analysis originated from various subcellular localizations including those of nontargeted organelles such as the nucleus, vacuole, chloroplast, and mitochondria. The high sensitivity of LC-MS/MS for protein identification is advantageous, allowing us to detect very small amounts of proteins. However, this sensitivity also poses a potential challenge as it increases the likelihood of detecting cross-contamination with nontargeted proteins during the immunoprecipitation process. This issue is not unique to our study as other protein identification methods face similar challenges.[18,72,73] In our case, it is possible that certain organelles may interact with the magnetic beads or antibodies used in the immunoprecipitation process, leading to the identification of nontargeted proteins. This cross-contamination could arise from shared binding properties or nonspecific interactions, complicating the interpretation of the results. Nonetheless, in our case, we can eliminate certain protein IDs, which are known to be localized in the nontargeted organelles.

We identified several glycosyltransferases, which are enzymes directly involved in cell wall polysaccharide synthesis, among other proteins associated with the cell wall, such as the UDP-xylose transporter, beta-glucosidase 6, beta-xylosidase, and PHGAP1. We conducted yeast-two-hybrid assays to validate interactions among the identified protein IDs, however, no direct interactions were observed. Alternative methods to verify these interactions are required. One potential approach could be to use the luciferase protein complementation assay, which has been employed to study protein interaction networks for XyG biosynthesis enzymes in the Golgi.[74] To compare our results with existing studies related to cell wall biosynthesis, we examined other reported proteins for protein interactions, immunoprecipitations, and proteomic analyses, such as Zhou et al.,[17] Parsons et al.[18] and Atmodjo et al.[20] However, we did not find a match between the proteins identified in our work and the data from these studies. Moreover, we investigated whether our protein IDs possessed the Lewis A glycans for proteins involved in cell wall biosynthesis,[75] but none of our identified proteins showed a match with them. Thus, it is probable that our approach has identified specific proteins associated with different polysaccharides, in which they may be present in low abundance and have not been previously detected in other studies.

Based on data from protein interaction databases, At5g22290 stands out as a hub protein interacting with numerous proteins related to cell wall biosynthesis. We observed connections between At5g22290 and cell wall-

https://doi.org/10.1021/acsomega.4c00534
ACS Omega 2024, 9, 31438−31454

associated proteins, including cellulose synthase-like proteins, arabinogalactan proteins, glycosyl hydrolases, pectin methylesterase inhibitors, and nucleotide sugar transporters. Furthermore, At5g22290 indirectly interacted with other proteins linking membrane and vesicle trafficking proteins with cell wall polysaccharides, including XyG, GX, and GM (Figure 7). No interactions were found for glycosyltransferases. Furthermore, we observed that many proteins, as per the protein interaction databases, interact with protein degradation factors. However, this does not necessarily mean that degradation was occurring during our analysis. Instead, these results suggest that these proteins may interact with protein degradation components under specific conditions for apoplastic delivery.

We note that our approach differed from previous reports on immunoprecipitation, particularly with regard to Golgi and GAUT complex pull down studies.[20] Those studies focused on pulling protein complexes at early stages of the biosynthesis, while our approach captures fully formed wall epitopes representing later stages of biosynthesis. Interestingly, our protein interaction analysis revealed interconnections between proteins associated with hemicelluloses and pectins. Our findings suggest that hemicellulose and pectin polymers may be present in the Golgi in close proximity to one another (Figure 7). However, it is important to acknowledge that our method makes it difficult to determine whether the captured epitopes originate from the Golgi or from Golgi derived vesicles.

Zhang and Staehelin[76] as well as Young et al.[77] have demonstrated that XyGs and pectins are synthesized within the Golgi stacks. Moore et al.[78] provided insight into the organization of different assembly pathways including glycoproteins and complex polysaccharides within the Golgi stacks. Polysaccharides and glycoproteins traverse through cisternae and are then packed into secretory vesicles to be transported to the trans-Golgi network. A study by Meents et al.[79] investigated xylan biosynthesis in the Golgi and found that the backbone synthesis enzyme, IRX9, predominantly localizes to the ring of the inner margins of medial cisternae, while the xylan products accumulate at the margins of trans−cisternae and the trans-Golgi network. Similarly, a subcompartment localization study of XyG biosynthesis enzymes indicated their presence in the cis- and medial- cisternae.[80] This discrepancy in the location of synthesis enzymes and final products may explain why our immunoprecipitation approach did not yield a higher number of glycosyltransferases, as the localization of the synthetic enzymes is different from that of the final products recognized by the glycan antibodies. Since cell wall polysaccharides are enriched in the trans-Golgi network,[81] it is plausible for proteins associated with a specific polysaccharide to be detected by other glycan-specific antibodies. Moreover, the presence of protein interaction networks representing associations with different matrix polysaccharides could suggest a shared location of these polysaccharides during the downstream biosynthesis in the Golgi, and potentially within secretory vesicles as well (Figure 7). This shared localization may play a role in the intricate process of polysaccharide biosynthesis and trafficking within the plant cell.

In recent years, several essential players involved in matrix polysaccharide biosynthesis have been discovered beyond the well-known glycosyltransferases responsible for their synthesis. Notably, a number of proteins localized in the Golgi network have been identified, each playing a crucial role in cell wall biosynthesis. For instance, MSR accessory proteins have been found to be important for mannan biosynthesis.[82,83] Additionally, CGR3 has been shown to influence the methyl esterification of HGA, and its identification was facilitated through coexpression analysis with cell wall synthesis genes.[84] The manganese transporter PML3 regulates plant growth through Golgi glycosylation and cell wall biosynthesis.[85] Similarly, BICAT3 is involved in matrix polysaccharide biosynthesis, with Mn being necessary for the normal cell wall biosynthesis process, likely without direct interactions with other biosynthesis enzymes. ER-localized cell wall-modifying enzymes, such as RWA2, are required for unspecifically acetylated cell wall polysaccharides.[86] In this study, we present a list of putative cell wall-related proteins involved in cell wall biosynthesis. In particular, we show through mutant studies that At3g22460 and At2g43700 knockouts show changes in polysaccharide composition, suggesting their role related to biosynthesis of XyG and GX, respectively.

Immunoprecipitation typically requires selecting a specific bait protein to capture nearby interacting proteins. This can be challenging when searching for unknown proteins involved in plant cell wall biosynthesis. Glycosyltransferases and glycan synthases are key targets for cell wall polysaccharide biosynthesis, but studying them using immunoprecipitation is difficult as they are membrane bound or membrane spanning proteins.[87] However, our approach, pulling the whole polysaccharide molecule with cross-linkers, broadens the targets to the polysaccharide itself rather than specific protein baits, eliminating the need to select specific protein baits and also avoiding the need for expression constructs or transformation. By using cross-linkers, we can explore additional proteins that may be localized in close proximity to the targeted polysaccharide. This method allows us to isolate proteins related to matrix polysaccharides throughout their biosynthesis, starting from a stage recognized by the antibody to their delivery in vesicles. Furthermore, our approach using glycan antibodies can be applied to directly targeting various polysaccharides based on the available antibodies. Over 200 cell wall antibodies recognizing 78 cell wall epitopes have been produced.[88] In summary, our method offers a means of studying cell wall polysaccharide biosynthesis and associated proteins, providing advantages over traditional immunoprecipitation techniques. Our study provides a list of putative proteins associated with the four different matrix polysaccharides for further investigation.

■ ASSOCIATED CONTENT

Data Availability Statement

All data generated and used in this study are available as Supporting Information for this article.

Supporting Information

The Supporting Information is available free of charge at https://pubs.acs.org/doi/10.1021/acsomega.4c00534.

DeepArappi interaction (XLSX)

ATMAD protein interaction (XLSX)

Coexpression RNA-seq database (XLSX)

Figure S1. Full-length gels for T-DNA insertion lines. Table S1. Primer sequences for identifications of T-DNA insertion lines. Table S2. Protein identifications of glycan-protein (GP), glycan-protein and protein−protein (GP+PP) cross-linked and no cross-linked immunoprecipitation via cell wall specific antibodies.

https://doi.org/10.1021/acsomega.4c00534
ACS Omega 2024, 9, 31438−31454

Peptide sequences and matching positions to *Arabidopsis* proteins are presented. Table S3. Lists of proteins used for yeast-two-hybrid assays with. Protein IDs within each antibody groups were assayed in all combination. Protein IDs with self-interaction based on yeast-two-hybrid assays are indicated using asterisks (PDF)

AUTHOR INFORMATION

Corresponding Author

Supachai Vuttipongchaikij − *Department of Genetics, Faculty of Science, Kasetsart University, Bangkok 10900, Thailand; Center of Advanced Studies for Tropical Natural Resources, Kasetsart University, Bangkok 10900, Thailand; Omics Center for Agriculture, Bioresources, Food and Health, Kasetsart University (OmiKU), Bangkok 10900, Thailand;* orcid.org/0000-0002-1194-3552; Email: supachai.v@ku.th

Authors

Pitchaporn Wannitikul − *Department of Genetics, Faculty of Science, Kasetsart University, Bangkok 10900, Thailand*

Issariya Dachphun − *Department of Genetics, Faculty of Science, Kasetsart University, Bangkok 10900, Thailand*

Jenjira Sakulkoo − *Department of Genetics, Faculty of Science, Kasetsart University, Bangkok 10900, Thailand*

Anongpat Suttangkakul − *Department of Genetics, Faculty of Science, Kasetsart University, Bangkok 10900, Thailand; Center of Advanced Studies for Tropical Natural Resources, Kasetsart University, Bangkok 10900, Thailand; Omics Center for Agriculture, Bioresources, Food and Health, Kasetsart University (OmiKU), Bangkok 10900, Thailand*

Passorn Wonnapinij − *Department of Genetics, Faculty of Science, Kasetsart University, Bangkok 10900, Thailand; Center of Advanced Studies for Tropical Natural Resources, Kasetsart University, Bangkok 10900, Thailand; Omics Center for Agriculture, Bioresources, Food and Health, Kasetsart University (OmiKU), Bangkok 10900, Thailand*

Rachael Simister − *CNAP, Department of Biology, University of York, Heslington, York YO10 5DD, United Kingdom*

Leonardo D. Gomez − *CNAP, Department of Biology, University of York, Heslington, York YO10 5DD, United Kingdom*

Complete contact information is available at: https://pubs.acs.org/10.1021/acsomega.4c00534

Author Contributions

S.V. and P.Wan. conceived the project and designed experiments. P.Wan., I.D., J.S., A.S., P.Wo., R.S., and L.G. performed the experiments and analyzed the data. S.V., P.Wan., and P.Wo. prepared the Figures and Tables and wrote the manuscript. L.G. revised the manuscript. All authors have approved the final version.

Notes

The authors declare no competing financial interest.

ACKNOWLEDGMENTS

This work was supported by the National Research Council of Thailand: NRCT5-RSA63002-02; The Office of the Ministry of Higher Education, Science, Research and Innovation; and the Thailand Science Research and Innovation through the Kasetsart University Reinventing University Program 2021, Kasetsart University Research and Development Institute (KURDI). We are also grateful for the support of the Biotechnology and Biological Sciences Research Council (grant reference BB/Y51424X/1 - BBSRC International Institutional Sponsorship Awards Tranche 1 York). P.Wan. was supported by Science Achievement Scholarship of Thailand (SAST). P.Wo. was supported by NRCT-N42A650286.

REFERENCES

(1) Zhang, B.; Gao, Y.; Zhang, L.; Zhou, Y. The plant cell wall: Biosynthesis, construction, and functions. *J. Integr. Plant Biol.* **2021**, *63* (1), 251−272.

(2) Drakakaki, G. Polysaccharide deposition during cytokinesis: challenges and future perspectives. *Plant Science* **2015**, *236*, 177−184.

(3) Cosgrove, D. J. Catalysts of plant cell wall loosening. *F1000Research* **2016**, *5*, 119.

(4) Van de Meene, A. M. L.; Doblin, M. S.; Bacic, A. The plant secretory pathway seen through the lens of the cell wall. *Protoplasma* **2017**, *254*, 75−94.

(5) Hoffmann, N.; King, S.; Samuels, A. L.; McFarlane, H. E. Subcellular coordination of plant cell wall synthesis. *Dev. Cell.* **2021**, *56* (7), 933−948.

(6) Amos, R. A.; Mohnen, D. Critical review of plant cell wall matrix polysaccharide glycosyltransferase activities verified by heterologous protein expression. *Front. Plant Sci.* **2019**, *10*, 915.

(7) Zhang, Y.; Yu, J.; Wang, X.; Durachko, D. M.; Zhang, S.; Cosgrove, D. J. Molecular insights into the complex mechanics of plant epidermal cell walls. *Science* **2021**, *372* (6543), 706−711.

(8) Kirui, A.; Du, J.; Zhao, W.; Barnes, W.; Kang, X.; Anderson, C. T.; Xiao, C.; Wang, T. A pectin methyltransferase modulates polysaccharide dynamics and interactions in Arabidopsis primary cell walls: Evidence from solid-state NMR. *Carbohydr. Polym.* **2021**, *270*, No. 118370.

(9) Fry, S. C.; York, W. S.; Albersheim, P.; Darvill, A.; Hayashi, T.; Joseleau, J. P.; Kato, Y.; Lorences, E. P.; Maclachlan, G. A.; McNeil, M.; Mort, A. J.; et al. An unambiguous nomenclature for xyloglucan-derived oligosaccharides. *Physiologia Plantarum* **1993**, *89* (1), 1−3.

(10) Scheller, H. V.; Ulvskov, P. Hemicelluloses. *Annual review of plant biology* **2010**, *61*, 263−289.

(11) Ishida, K.; Ohba, Y.; Yoshimi, Y.; Wilson, L. F.; Echevarría-Poza, A.; Yu, L.; Iwai, H.; Dupree, P. Differing structures of galactoglucomannan in eudicots and non-eudicot angiosperms. *PLoS One* **2023**, *18* (12), No. e0289581.

(12) Mohnen, D. Pectin structure and biosynthesis. *Current opinion in plant biology* **2008**, *11* (3), 266−277.

(13) Harholt, J.; Suttangkakul, A.; Vibe Scheller, H. Biosynthesis of pectin. *Plant physiology* **2010**, *153* (2), 384−395.

(14) Schultink, A.; Naylor, D.; Dama, M.; Pauly, M. The role of the plant-specific ALTERED XYLOGLUCAN9 protein in Arabidopsis cell wall polysaccharide O-acetylation. *Plant Physiology* **2015**, *167* (4), 1271−1283.

(15) Temple, H.; Phyo, P.; Yang, W.; Lyczakowski, J. J.; Echevarría-Poza, A.; Yakunin, I.; Parra-Rojas, J. P.; Terrett, O. M.; Saez-Aguayo, S.; Dupree, R.; Orellana, A.; et al. Golgi-localized putative S-adenosyl methionine transporters required for plant cell wall polysaccharide methylation. *Nature Plants* **2022**, *8* (6), 656−669.

(16) Du, J.; Kirui, A.; Huang, S.; Wang, L.; Barnes, W. J.; Kiemle, S. N.; Zheng, Y.; Rui, Y.; Ruan, M.; Qi, S.; Kim, S. H.; et al. Mutations in the pectin methyltransferase QUASIMODO2 influence cellulose biosynthesis and wall integrity in Arabidopsis. *Plant Cell* **2020**, *32* (11), 3576−3597.

(17) Zhou, C.; Yin, Y.; Dam, P.; Xu, Y. Identification of Novel Proteins Involved in Plant Cell-Wall Synthesis Based on Protein-Protein Interaction Data. *J. Proteome Res.* **2010**, *9* (10), 5025−5037.

(18) Parsons, H. T.; Christiansen, K.; Knierim, B.; Carroll, A.; Ito, J.; Batth, T. S.; Smith-Moritz, A. M.; Morrison, S.; McInerney, P.; Hadi, M. Z.; Auer, M.; et al. Isolation and proteomic characterization of the

Arabidopsis Golgi defines functional and novel components involved in plant cell wall biosynthesis. *Plant Physiol* **2012**, *159* (1), 12−26.
(19) Cai, B.; Li, C. H.; Huang, J. Systematic identification of cell-wall related genes in Populus based on analysis of functional modules in co-expression network. *PloS One* **2014**, *9* (4), No. e95176.
(20) Atmodjo, M. A.; Sakuragi, Y.; Zhu, X.; Burrell, A. J.; Mohanty, S. S.; Atwood III, J. A.; Orlando, R.; Scheller, H. V.; Mohnen, D. Galacturonosyltransferase (GAUT) 1 and GAUT7 are the core of a plant cell wall pectin biosynthetic homogalacturonan: galacturonosyltransferase complex. *Proc. Natl. Acad. Sci. U. S. A.* **2011**, *108* (50), 20225−20230.
(21) Albenne, C.; Canut, H.; Jamet, E. Plant cell wall proteomics: the leadership of Arabidopsis thaliana. *Front. Plant Sci.* **2013**, *4*, 111.
(22) Wu, F. H.; Shen, S. C.; Lee, L. Y.; Lee, S. H.; Chan, M. T.; Lin, C. S. Tape-Arabidopsis Sandwich-a simpler Arabidopsis protoplast isolation method. *Plant Methods* **2009**, *5*, 1−10.
(23) Zheng, J.; Yang, X.; Huang, Y.; Yang, S.; Wuchty, S.; Zhang, Z. Deep learning-assisted prediction of protein−protein interactions in Arabidopsis thaliana. *Plant J.* **2023**, *114* (4), 984−994.
(24) Lan, Y.; Sun, R.; Ouyang, J.; Ding, W.; Kim, M. J.; Wu, J.; Li, Y.; Shi, T. AtMAD: Arabidopsis thaliana multi-omics association database. *Nucleic Acids Res.* **2021**, *49* (D1), D1445−D1451.
(25) Zhang, H.; Zhang, F.; Yu, Y.; Feng, L. I.; Jia, J.; Liu, B. O.; Li, B.; Guo, H.; Zhai, J. A comprehensive online database for exploring∼20,000 public Arabidopsis RNA-seq libraries. *Mol. Plant* **2020**, *13* (9), 1231−1233.
(26) Csardi, G.; Nepusz, T. The igraph software package for complex network research. *Inter Journal, complex systems* **2006**, *1695* (5), 1−9.
(27) Pettolino, F. A.; Walsh, C.; Fincher, G. B.; Bacic, A. Determining the polysaccharide composition of plant cell walls. *Nature protocols* **2012**, *7* (9), 1590−1607.
(28) Jones, L.; Milne, J. L.; Ashford, D.; McQueen-Mason, S. J. Cell wall arabinan is essential for guard cell function. *Proc. Natl. Acad. Sci. U. S. A.* **2003**, *100* (20), 11783−11788.
(29) Morse, E. E. Anthrone in estimating low concentration of sucrose. *Anal. Chem.* **1947**, *19*, 1012−1013.
(30) Saeman, J. F. Kinetics of wood saccharification-hydrolysis of cellulose and decomposition of sugars in dilute acid at high temperature. *Industrial & Engineering Chemistry* **1945**, *37* (1), 43−52.
(31) Gomez, L. D.; Whitehead, C.; Barakate, A.; Halpin, C.; McQueen-Mason, S. J. Automated saccharification assay for determination of digestibility in plant materials. *Biotechnol. Biofuels* **2010**, *3*, 1−12.
(32) Whitehead, C.; Gomez, L. D.; McQueen-Mason, S. J. The analysis of saccharification in biomass using an automated high-throughput method. In *Methods in enzymology*; Academic Press, 2012; Vol. *510*, pp 37−50.
(33) Anthon, G. E.; Barrett, D. M. Determination of reducing sugars with 3-methyl-2-benzothiazolinonehydrazone. *Analytical biochemistry* **2002**, *305* (2), 287−289.
(34) Marcus, S. E.; Verhertbruggen, Y.; Hervé, C.; Ordaz-Ortiz, J. J.; Farkas, V.; Pedersen, H. L.; Willats, W. G.; Knox, J. P. Pectic homogalacturonan masks abundant sets of xyloglucan epitopes in plant cell walls. *BMC Plant Biol.* **2008**, *8* (1), 1−12.
(35) Cornuault, V.; Buffetto, F.; Rydahl, M. G.; Marcus, S. E.; Torode, T. A.; Xue, J.; Crépeau, M. J.; Faria-Blanc, N.; Willats, W. G.; Dupree, P.; Ralet, M. C.; et al. Monoclonal antibodies indicate low-abundance links between heteroxylan and other glycans of plant cell walls. *Planta* **2015**, *242* (6), 1321−1334.
(36) Marcus, S. E.; Blake, A. W.; Benians, T. A.; Lee, K. J.; Poyser, C.; Donaldson, L.; Leroux, O.; Rogowski, A.; Petersen, H. L.; Boraston, A.; Gilbert, H. J.; et al. Restricted access of proteins to mannan polysaccharides in intact plant cell walls. *Plant J.* **2010**, *64* (2), 191−203.
(37) Verhertbruggen, Y.; Marcus, S. E.; Haeger, A.; Ordaz-Ortiz, J. J.; Knox, J. P. An extended set of monoclonal antibodies to pectic homogalacturonan. *Carbohydr. Res.* **2009**, *344* (14), 1858−1862.
(38) Lee, J.; Tomasek, D.; Santos, T. M.; May, M. D.; Meuskens, I.; Kahne, D. Formation of a β-barrel membrane protein is catalyzed by the interior surface of the assembly machine protein BamA. *Elife* **2019**, *8*, No. e49787.
(39) Flack, C. E.; Parkinson, J. S. Structural signatures of Escherichia coli chemoreceptor signaling states revealed by cellular crosslinking. *Proc. Natl. Acad. Sci. U. S. A.* **2022**, *119* (28), No. e2204161119.
(40) Antar, H.; Soh, Y. M.; Zamuner, S.; Bock, F. P.; Anchimiuk, A.; Rios, P. D. L.; Gruber, S. Relief of ParB autoinhibition by parS DNA catalysis and recycling of ParB by CTP hydrolysis promote bacterial centromere assembly. *Sci. Adv.* **2021**, *7* (41), No. eabj2854.
(41) Nozawa, K.; Takizawa, Y.; Pierrakeas, L.; Sogawa-Fujiwara, C.; Saikusa, K.; Akashi, S.; Luk, E.; Kurumizaka, H. Cryo−electron microscopy structure of the H3-H4 octasome: A nucleosome-like particle without histones H2A and H2B. *Proc. Natl. Acad. Sci. U. S. A.* **2022**, *119* (45), No. e2206542119.
(42) Goyal, P.; Pandey, D.; Brünnert, D.; Hammer, E.; Zygmunt, M.; Siess, W. Cofilin oligomer formation occurs in vivo and is regulated by cofilin phosphorylation. *PLoS One* **2013**, *8* (8), No. e71769.
(43) Ishmael, S. S.; Ishmael, F. T.; Jones, A. D.; Bond, J. S. Protease domain glycans affect oligomerization, disulfide bond formation, and stability of the meprin A metalloprotease homo-oligomer. *J. Biol. Chem.* **2006**, *281* (49), 37404−37415.
(44) Gunning, A. P.; Bongaerts, R. J.; Morris, V. J. Recognition of galactan components of pectin by galectin-3. *FASEB J.* **2009**, *23* (2), 415−424.
(45) Hozumi, K.; Nomizu, M. Cell adhesion activity of peptides conjugated to polysaccharides. *Curr. Protoc. Cell Biol.* **2018**, *80* (1), No. e53.
(46) Yu, L.; Yoshimi, Y.; Cresswell, R.; Wightman, R.; Lyczakowski, J. J.; Wilson, L. F.; Ishida, K.; Stott, K.; Yu, X.; Charalambous, S.; Wurman-Rodrich, J.; et al. Eudicot primary cell wall glucomannan is related in synthesis, structure, and function to xyloglucan. *Plant Cell* **2022**, *34* (11), 4600−4622.
(47) Yamaguchi, C.; Takimoto, Y.; Ohkama-Ohtsu, N.; Hokura, A.; Shinano, T.; Nakamura, T.; Suyama, A.; Maruyama-Nakashita, A. Effects of cadmium treatment on the uptake and translocation of sulfate in Arabidopsis thaliana. *Plant Cell Physiol* **2016**, *57* (11), 2353−2366.
(48) Liu, X.; Wu, F. H.; Li, J. X.; Chen, J.; Wang, G. H.; Wang, W. H.; Hu, W. J.; Gao, L. J.; Wang, Z. L.; Chen, J. H.; Simon, M.; et al. Glutathione homeostasis and Cd tolerance in the Arabidopsis sultr1; 1-sultr1; 2 double mutant with limiting sulfate supply. *Plant Cell Rep* **2016**, *35*, 397−413.
(49) Shirzadian-Khorramabad, R.; Jing, H. C.; Everts, G. E.; Schippers, J. H.; Hille, J.; Dijkwel, P. P. A mutation in the cytosolic O-acetylserine (thiol) lyase induces a genome-dependent early leaf death phenotype in Arabidopsis. *BMC Plant Biol.* **2010**, *10*, 1−12.
(50) Birke, H.; De Kok, L. J.; Wirtz, M.; Hell, R. The role of compartment-specific cysteine synthesis for sulfur homeostasis during H2S exposure in Arabidopsis. *Plant Cell Physiol* **2015**, *56* (2), 358−367.
(51) Maeda, H.; Song, W.; Sage, T.; DellaPenna, D. Role of callose synthases in transfer cell wall development in tocopherol deficient Arabidopsis mutants. *Front. Plant Sci.* **2014**, *5*, 46.
(52) Sugita, M. An overview of pentatricopeptide repeat (PPR) proteins in the moss Physcomitrium patens and their role in organellar gene expression. *Plants* **2022**, *11* (17), 2279.
(53) Mangeon, A.; Pardal, R.; Menezes-Salgueiro, A. D.; Duarte, G. L.; de Seixas, R.; Cruz, F. P.; Cardeal, V.; Magioli, C.; Ricachenevsky, F. K.; Margis, R.; Sachetto-Martins, G. AtGRP3 is implicated in root size and aluminum response pathways in Arabidopsis. *PLoS One* **2016**, *11* (3), No. e0150583.
(54) Chien, P. S.; Chao, Y. T.; Chou, C. H.; Hsu, Y. Y.; Chiang, S. F.; Tung, C. W.; Chiou, T. J. Phosphate transporter PHT1; 1 is a key determinant of phosphorus acquisition in Arabidopsis natural accessions. *Plant Physiol* **2022**, *190* (1), 682−697.

https://doi.org/10.1021/acsomega.4c00534
ACS Omega 2024, 9, 31438−31454

(55) Zou, J. J.; Wei, F. J.; Wang, C.; Wu, J. J.; Ratnasekera, D.; Liu, W. X.; Wu, W. H. Arabidopsis calcium-dependent protein kinase CPK10 functions in abscisic acid- and Ca2+-mediated stomatal regulation in response to drought stress. *Plant Physiol* **2010**, *154* (3), 1232−1243.
(56) Meißner, D.; Albert, A.; Böttcher, C.; Strack, D.; Milkowski, C. The role of UDP-glucose: hydroxycinnamate glucosyltransferases in phenylpropanoid metabolism and the response to UV-B radiation in Arabidopsis thaliana. *Planta* **2008**, *228*, 663−674.
(57) Lauster, T.; Stoeckle, D.; Gabor, K.; Haller, T.; Krieger, N.; Lotz, P.; Mayakrishnan, R.; Späth, E.; Zimmermann, S.; Livanos, P.; Mueller, S. Arabidopsis pavement cell shape formation involves spatially confined ROPGAP regulators. *Curr. Biol.* **2022**, *32* (3), 532−544.
(58) Beathard, C.; Mooney, S.; Al-Saharin, R.; Goyer, A.; Hellmann, H. Characterization of Arabidopsis thaliana R2R3 S23 MYB transcription factors as novel targets of the ubiquitin proteasome-pathway and regulators of salt stress and abscisic acid response. *Front. Plant Sci.* **2021**, *12*, No. 629208.
(59) Ebert, B.; Rautengarten, C.; Guo, X.; Xiong, G.; Stonebloom, S.; Smith-Moritz, A. M.; Herter, T.; Chan, L. J. G.; Adams, P. D.; Petzold, C. J.; Pauly, M.; et al. Identification and characterization of a Golgi-localized UDP-xylose transporter family from Arabidopsis. *Plant Cell* **2015**, *27* (4), 1218−1227.
(60) Caffall, K. H.; Pattathil, S.; Phillips, S. E.; Hahn, M. G.; Mohnen, D. Arabidopsis thaliana T-DNA mutants implicate GAUT genes in the biosynthesis of pectin and xylan in cell walls and seed testa. *Mol. Plant* **2009**, *2* (5), 1000−1014.
(61) Klein, P.; Seidel, T.; Stöcker, B.; Dietz, K. J. The membrane-tethered transcription factor ANAC089 serves as a redox-dependent suppressor of stromal ascorbate peroxidase gene expression. *Front. Plant Sci.* **2012**, *3*, 247.
(62) Kang, X.; Li, W.; Zhou, Y.; Ni, M. A WRKY transcription factor recruits the SYG1-like protein SHB1 to activate gene expression and seed cavity enlargement. *PLoS Genet* **2013**, *9* (3), No. e1003347.
(63) Pietra, S.; Gustavsson, A.; Kiefer, C.; Kalmbach, L.; Hörstedt, P.; Ikeda, Y.; Stepanova, A. N.; Alonso, J. M.; Grebe, M. Arabidopsis SABRE and CLASP interact to stabilize cell division plane orientation and planar polarity. *Nat. Commun.* **2013**, *4* (1), 2779.
(64) Ojangu, E. L.; Tanner, K.; Pata, P.; Järve, K.; Holweg, C. L.; Truve, E.; Paves, H. Myosins XI-K, XI-1, and XI-2 are required for the development of pavement cells, trichomes, and stigmatic papillae in Arabidopsis. *BMC Plant Biol.* **2012**, *12* (1), 81.
(65) Leshem, Y.; Golani, Y.; Kaye, Y.; Levine, A. Reduced expression of the v-SNAREs AtVAMP71/AtVAMP7C gene family in Arabidopsis reduces drought tolerance by suppression of abscisic acid-dependent stomatal closure. *J. Exp. Bot.* **2010**, *61* (10), 2615−2622.
(66) Leshem, Y.; Melamed-Book, N.; Cagnac, O.; Ronen, G.; Nishri, Y.; Solomon, M.; Cohen, G.; Levine, A. Suppression of Arabidopsis vesicle-SNARE expression inhibits fusion of H2O2-containing vesicles with tonoplast and increases salt tolerance. *Proc. Natl. Acad. Sci. U. S. A.* **2006**, *103* (47), 18008−18013.
(67) Haydon, M. J.; Kawachi, M.; Wirtz, M.; Hillmer, S.; Hell, R.; Krämer, U. Vacuolar nicotianamine has critical and distinct roles under iron deficiency and for zinc sequestration in Arabidopsis. *Plant Cell* **2012**, *24* (2), 724−737.
(68) Lauster, T.; Stoeckle, D.; Gabor, K.; Haller, T.; Krieger, N.; Lotz, P.; Mayakrishnan, R.; Späth, E.; Zimmermann, S.; Livanos, P.; Mueller, S. Arabidopsis pavement cell shape formation involves spatially confined ROPGAP regulators. *Curr. Biol.* **2022**, *32* (3), 532−544.
(69) Oda, Y.; Fukuda, H. Rho of plant GTPase signaling regulates the behavior of Arabidopsis kinesin-13A to establish secondary cell wall patterns. *Plant Cell* **2013**, *25* (11), 4439−4450.
(70) Sugiyama, Y.; Nagashima, Y.; Wakazaki, M.; Sato, M.; Toyooka, K.; Fukuda, H.; Oda, Y. A Rho-actin signaling pathway shapes cell wall boundaries in Arabidopsis xylem vessels. *Nat. Commun.* **2019**, *10* (1), 468.
(71) Alavarse, A. C.; Frachini, E. C. G.; da Silva, R. L. C. G.; Lima, V. H.; Shavandi, A.; Petri, D. F. S. Crosslinkers for polysaccharides and proteins: Synthesis conditions, mechanisms, and crosslinking efficiency, a review. *Int. J. Biol. Macromol.* **2022**, *202*, 558−596.
(72) Fasimoye, R.; Dong, W.; Nirujogi, R. S.; Rawat, E. S.; Iguchi, M.; Nyame, K.; Phung, T. K.; Bagnoli, E.; Prescott, A. R.; Alessi, D. R.; Abu-Remaileh, M. Golgi-IP, a tool for multimodal analysis of Golgi molecular content. *Proc. Natl. Acad. Sci. U. S. A.* **2023**, *120* (20), No. e2219953120.
(73) Xu, S. L.; Shrestha, R.; Karunadasa, S. S.; Xie, P. Q. Proximity labeling in plants. *Annu. Rev. Plant Biol.* **2023**, *74*, 285−312.
(74) Lund, C. H.; Bromley, J. R.; Stenbæk, A.; Rasmussen, R. E.; Scheller, H. V.; Sakuragi, Y. A reversible Renilla luciferase protein complementation assay for rapid identification of protein−protein interactions reveals the existence of an interaction network involved in xyloglucan biosynthesis in the plant Golgi apparatus. *J. Exp. Bot.* **2015**, *66* (1), 85−97.
(75) Beihammer, G.; Maresch, D.; Altmann, F.; Van Damme, E. J.; Strasser, R. Lewis A glycans are present on proteins involved in cell wall biosynthesis and appear evolutionarily conserved among natural Arabidopsis thaliana accessions. *Front. Plant Sci.* **2021**, *12*, No. 630891.
(76) Zhang, G. F.; Staehelin, L. A. Functional compartmentation of the Golgi apparatus of plant cells: immunocytochemical analysis of high-pressure frozen-and freeze-substituted sycamore maple suspension culture cells. *Plant Physiol* **1992**, *99* (3), 1070−1083.
(77) Young, R. E.; McFarlane, H. E.; Hahn, M. G.; Western, T. L.; Haughn, G. W.; Samuels, A. L. Analysis of the Golgi apparatus in Arabidopsis seed coat cells during polarized secretion of pectin-rich mucilage. *Plant Cell* **2008**, *20* (6), 1623−1638.
(78) Moore, P. J.; Swords, K. M.; Lynch, M. A.; Staehelin, L. A. Spatial organization of the assembly pathways of glycoproteins and complex polysaccharides in the Golgi apparatus of plants. *J. Cell Biol.* **1991**, *112* (4), 589−602.
(79) Meents, M. J.; Motani, S.; Mansfield, S. D.; Samuels, A. L. Organization of xylan production in the Golgi during secondary cell wall biosynthesis. *Plant Physiol* **2019**, *181* (2), 527−546.
(80) Chevalier, L.; Bernard, S.; Ramdani, Y.; Lamour, R.; Bardor, M.; Lerouge, P.; Follet-Gueye, M. L.; Driouich, A. Subcompartment localization of the side chain xyloglucan-synthesizing enzymes within Golgi stacks of tobacco suspension-cultred cells. *Plant J.* **2010**, *64* (6), 977−989.
(81) Wilkop, T.; Pattathil, S.; Ren, G.; Davis, D. J.; Bao, W.; Duan, D.; Peralta, A. G.; Domozych, D. S.; Hahn, M. G.; Drakakaki, G. A hybrid approach enabling large-scale glycomic analysis of post-Golgi vesicles reveals a transport route for polysaccharides. *Plant Cell* **2019**, *31* (3), 627−644.
(82) Wang, Y.; Mortimer, J. C.; Davis, J.; Dupree, P.; Keegstra, K. Identification of an additional protein involved in mannan biosynthesis. *Plant J.* **2013**, *73* (1), 105−117.
(83) Voiniciuc, C.; Dama, M.; Gawenda, N.; Stritt, F.; Pauly, M. Mechanistic insights from plant heteromannan synthesis in yeast. *Proc. Natl. Acad. Sci. U. S. A.* **2019**, *116* (2), 522−527.
(84) Held, M. A.; Be, E.; Zemelis, S.; Withers, S.; Wilkerson, C.; Brandizzi, F. CGR3: a Golgi-localized protein influencing homogalacturonan methylesterification. *Mol. Plant* **2011**, *4* (5), 832−844.
(85) Yang, C. H.; Wang, C.; Singh, S.; Fan, N.; Liu, S.; Zhao, L.; Cao, H.; Xie, W.; Yang, C.; Huang, C. F. Golgi-localised manganese transporter PML3 regulates Arabidopsis growth through modulating Golgi glycosylation and cell wall biosynthesis. *New Phytol* **2021**, *231* (6), 2200−2214.
(86) Manabe, Y.; Nafisi, M.; Verhertbruggen, Y.; Orfila, C.; Gille, S.; Rautengarten, C.; Cherk, C.; Marcus, S. E.; Somerville, S.; Pauly, M.; Knox, J. P.; et al. Loss-of-function mutation of REDUCED WALL ACETYLATION2 in Arabidopsis leads to reduced cell wall acetylation and increased resistance to Botrytis cinerea. *Plant Physiol* **2011**, *155* (3), 1068−1078.

https://doi.org/10.1021/acsomega.4c00534
ACS Omega 2024, 9, 31438−31454

(87) Amos, R. A.; Mohnen, D. Critical review of plant cell wall matrix polysaccharide glycosyltransferase activities verified by heterologous protein expression. *Front. Plant Sci.* **2019**, *10*, 915.
(88) Ruprecht, C.; Bartetzko, M. P.; Senf, D.; Dallabernadina, P.; Boos, I.; Andersen, M. C.; Kotake, T.; Knox, J. P.; Hahn, M. G.; Clausen, M. H.; Pfrengle, F. A synthetic glycan microarray enables epitope mapping of plant cell wall glycan-directed antibodies. *Plant Physiol* **2017**, *175* (3), 1094−1104.

https://doi.org/10.1021/acsomega.4c00534
ACS Omega 2024, 9, 31438−31454